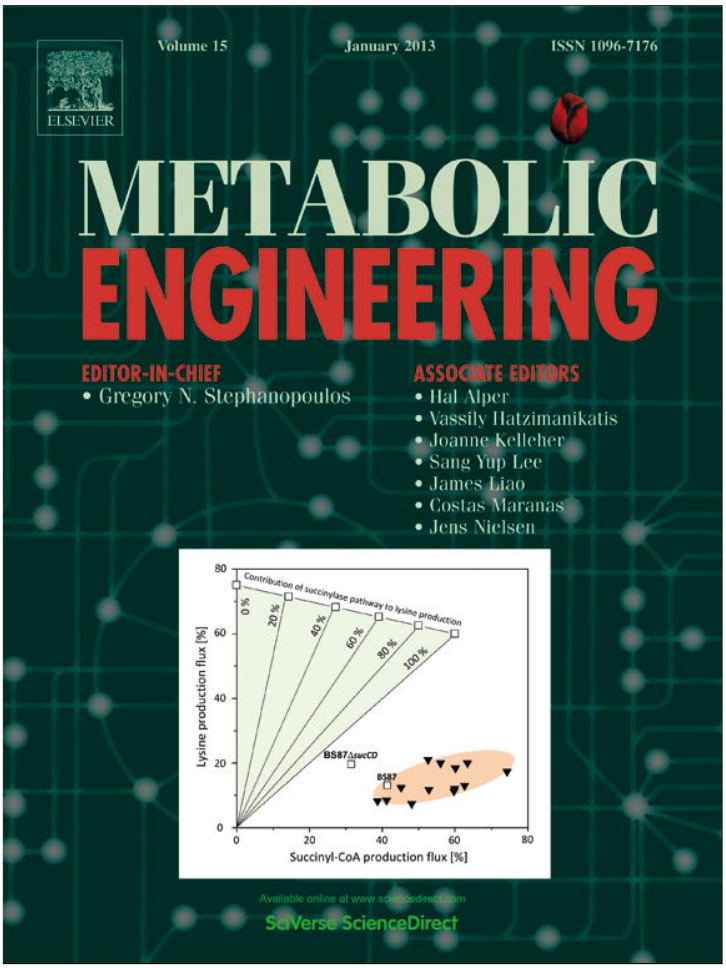

Metabolic Engineering 15 (2013) 98–112

Contents lists available at SciVerse ScienceDirect

Metabolic Engineering

journal homepage: www.elsevier.com/locate/ymben

Engineering an anaerobic metabolic regime in *Pseudomonas putida* KT2440 for the anoxic biodegradation of 1,3-dichloroprop-1-ene

Pablo I. Nikel, Víctor de Lorenzo *

Systems and Synthetic Biology Program, Centro Nacional de Biotecnología (CNB-CSIC), Madrid 28049, Spain

ARTICLE INFO

Article history:
Received 29 August 2012
Accepted 21 September 2012
Available online 10 November 2012

Keywords:
Pseudomonas putida
Limited oxygen supply
Redox and energy balance
Biocatalysis
Organochloride
Biodegradation

ABSTRACT

Pseudomonas putida KT2440, a microbial cell factory of reference for industrial whole-cell biocatalysis, is unable to support biochemical reactions that occur under anoxic conditions, limiting its utility for a large number of relevant biotransformations. Unlike (facultative) anaerobes, *P. putida* resorts to NADH oxidation *via* an oxic respiratory chain and completely lacks a true fermentation metabolism. Therefore, it cannot achieve the correct balances of energy and redox couples (i.e., ATP/ADP and NADH/NAD^+) that are required to sustain an O_2-free lifestyle. To overcome this state of affairs, the acetate kinase (*ackA*) gene of the facultative anaerobe *Escherichia coli* and the pyruvate decarboxylase (*pdc*) and alcohol dehydrogenase II (*adhB*) genes of the aerotolerant *Zymomonas mobilis* were knocked-in to a wild-type *P. putida* strain. Biochemical and genetic assays showed that conditional expression of the entire enzyme set allowed the engineered bacteria to adopt an anoxic regime that maintained considerable metabolic activity. The resulting strain was exploited as a host for the heterologous expression of a 1,3-dichloroprop-1-ene degradation pathway recruited from *Pseudomonas pavonaceae* 170, enabling the recombinants to degrade this recalcitrant chlorinated compound anoxically. These results underscore the value of *P. putida* as a versatile agent for biotransformations able to function at progressively lower redox statuses.

1. Introduction

Bacteria of the genus *Pseudomonas*, like most heterotrophic bacteria, oxidise organic carbon sources through the Entner–Doudoroff pathway and the tricarboxylic acid cycle (Fig. 1; Blank et al., 2008; Chavarría et al., 2012; Fuhrer et al., 2005). Several of the oxidative steps in these metabolic processes are coupled to the reduction of NAD^+ to NADH, and NADH must be re-oxidised so that these pathways can proceed and generate anabolic precursors needed for bacterial growth. In pseudomonads, the primary mechanism by which this process is accomplished is the reduction of one of the NADH dehydrogenases at the start of the respiratory chain, which ultimately transfers the electrons to O_2 or NO_3^-. *Pseudomonas putida* KT2440, one of the most widespread species and strains used in industrial and environmental biocatalysis (Poblete-Castro et al., 2012), strictly relies on O_2-dependent reactions to generate energy and, for that reason, has been deemed an obligate aerobic bacterium (Nelson et al., 2002; Nogales et al., 2008). The adoption of such a metabolic regime clearly limits the applications of *P. putida* in a number of biotransformations for either adding value to given substrates or for their complete mineralisation to CO_2 and H_2O. Target compounds of this sort include (but are certainly not limited to) many synthetic organohalide chemicals. The use of organohalides peaked in the 1960s because of their exceptional properties, but their resistance to both chemical and biological metabolism has become a paradigm of difficult-to-eliminate anthropogenic molecules (Fetzner, 1998); organohalides accumulation in soils being particularly worrisome (Lee et al., 1998). Apart from their intrinsic resistance, a single chlorinated compound can contaminate both the oxic and anoxic zones of the same soil or H_2O column (Schöler et al., 2003). This makes it very difficult to employ the same biocatalyst under different redox conditions that normally coexist in the same afflicted site.

Typical biodegradation mechanisms of organohalides include oxidation, reduction, substitution, intramolecular substitution, dehydrohalogenation, hydration, and methyl-transfer reactions (Belkin, 1992; Castro, 1977). In addition to the specific enzymes that catalyse dehalogenation steps (i.e., dehalogenases), the carbon–halogen bond can also be cleaved spontaneously *via* production of unstable metabolites or by spontaneous reactions. Oxidative dehalogenations are catalysed by mono- and dioxygenases in reactions that incorporate either one or two oxygen atoms from O_2 into the organic substrate skeleton (de Jong and Dijkstra, 2003; Janssen, 2004; Keuning et al., 1985). Oxidative

* Correspondence to: Systems and Synthetic Biology Program Centro Nacional de BiotecnologÚa (CNB-CSIC) Darwin 3, Campus de Cantoblanco Madrid 28049, Spain. Fax: +34 91 585 4506.
E-mail address: vdlorenzo@cnb.csic.es (V. de Lorenzo).

1096-7176/$ - see front matter © 2012 Elsevier Inc. All rights reserved.
http://dx.doi.org/10.1016/j.ymben.2012.09.006

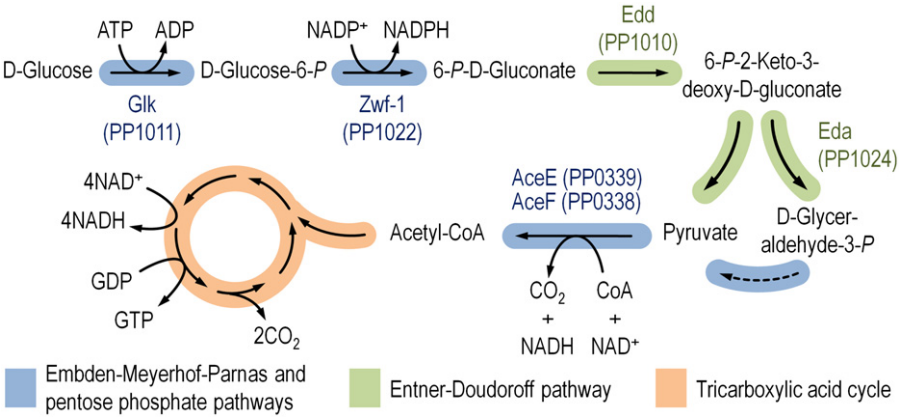

Fig. 1. Simplified scheme of the pathways involved in D-glucose catabolism in *P. putida* KT2440 under oxic growth conditions. After the initial phosphorylation of D-glucose, catalysed by glucokinase (Glk), the resulting D-glucose-6-*P* is channelled through the Entner–Doudoroff pathway (Edd/Eda) *via* its conversion into 6-*P*-D-gluconate and 6-*P*-2-keto-3-deoxy-D-gluconate to finally yield pyruvate and D-glyceraldehyde-3-*P*. D-Glucose can also be converted into D-gluconate, 2-keto-D-gluconate, and 6-*P*-2-keto-D-gluconate (not depicted), but these intermediates are ultimately converted into 6-*P*-D-gluconate and yield the same C3 compounds as mentioned before. Pyruvate is transformed into acetyl-coenzyme A (CoA) through the activity of the pyruvate dehydrogenase complex (AceEF and other components) in a NAD^+-dependent reaction. Although acetyl-CoA can meet different fates depending on further catabolic steps, it is mainly oxidised in the tricarboxylic acid cycle. The reducing equivalents therein produced as NADH are used as electron donors in the respiratory chain, thereby generating energy during the oxidative phosphorylation process. The main metabolic blocks involved in D-glucose catabolism are depicted in different colours, and the relevant enzymatic steps are identified in parentheses by means of their locus (PP) numbers as annotated by Nelson et al. (2002). The broken line connecting pyruvate and D-glyceraldehyde-3-*P* represents several metabolic steps. Redundant enzymes and branched pathways conducive to the same intermediates are not shown in this outline.

dehalogenation is thus restricted to oxic environments and is by far the most common mechanism of biological detoxification for these compounds (Janssen et al., 2001). As mentioned above, this situation restricts the efficient removal of toxic organohalides from soils where, most typically, a thin O_2-exposed outside boundary is immediately followed by a much larger anoxic subsurface. Although a number of denitrifying bacteria (e.g., *Ochrobactrum* and *Thauera*) are capable of degrading some halogenated aromatics (Häggblom et al., 2000; Häggblom and Young, 1999; Song et al., 2000), haloalkenes are not easily (if at all) degraded under anoxic conditions.

This work reports our efforts to conditionally transform the metabolic lifestyle of *P. putida* KT2440 from functioning under all-oxic growth conditions to anoxic conditions capable of sustaining biodegradation of the model organohalide 1,3-dichloroprop-1-ene (1,3-DCP) in the absence of O_2 or any externally added electron acceptor. The starting point was the search of current metabolic models to diagnose what parts of the extant network of this bacterium had to be re-factored to bring about the desired catalytic phenotype. Following the knock-in of various genes retrieved from facultative anaerobe and aerotolerant bacteria, one of the successful combinations was used as the metabolic foundation to host a haloalkane dehalogenase activity from *Pseudomonas pavonaceae* 170. As shown below, this approach resulted in a recombinant strain able to degrade 1,3-DCP under anoxic conditions. These results not only pave the way for expanding the catalytic repertoire of *P. putida* but also highlight the value of metabolic engineering to shift the functional window of one bacterium across various redox regimes as required for the production of biochemicals and biofuels under conditions with restricted O_2 supply.

2. Materials and methods

2.1. Bacterial strains and culture conditions

Bacterial strains and plasmids used in this study are listed in Table 1. *Escherichia coli* and *Pseudomonas* strains were routinely grown at 37 °C and 30 °C, respectively, in LB medium (containing 10 g l^{-1} tryptone, 10 g l^{-1} NaCl, and 5 g l^{-1} yeast extract) under oxic conditions (i.e., in Erlenmeyer flasks containing medium up to one-fifth of their nominal volume with agitation at 170 rpm). *E. coli* DH5α and CC118λ*pir* were used for routine cloning procedures and plasmid maintenance. *Zymomonas mobilis* subsp. *mobilis* DSM 424 was grown under anoxic conditions in *Zymomonas* medium (containing 10 g l^{-1} peptone, 10 g l^{-1} yeast extract, and 10 g l^{-1} D-glucose) at 30 °C using 16 × 125-mm Hungate tubes (BellCo Glass Inc., Vineland, NJ, USA) completely filled with the culture medium. Recombinant *P. putida* strains and *E. coli* BW25113 were grown in M9 minimal medium, containing 6 g l^{-1} Na_2HPO_4, 3 g l^{-1} KH_2PO_4, 1.4 g l^{-1} $(NH_4)_2SO_4$, 0.5 g l^{-1} NaCl, 0.2 g l^{-1} $MgSO_4 \cdot 7H_2O$, 5 mg l^{-1} thiamine · HCl, and 2.5 ml l^{-1} of a trace elements solution (Abril et al., 1989). A modified M9 medium (M9C) was used for anoxic biotransformations, containing the same salts as those described above but added with 0.3 g l^{-1} K_2SO_4 instead of NaCl and 2.5 g l^{-1} yeast extract (Becton & Dickinson Co., Sparks, MD, USA) as a source of vitamins. D-Glucose was added as the sole carbon source at 10 g l^{-1}. *P. putida* recombinants were first grown under oxic conditions up to mid-exponential phase [i.e., to an optical density measured at 600 nm (OD_{600}) of ca. 0.5–0.6], cells were spun at 5000 × *g* for 10 min, and the sediment was resuspended in an appropriate volume of fresh medium to adjust the OD_{600} to 1. The cell suspension was added with the corresponding inducer of gene expression and incubated at 30 °C under anoxic conditions in Hungate tubes filled up to 75% of the nominal volume with constant rotary agitation to prevent biomass sedimentation. The absence of O_2 was qualitatively checked by including 0.75 mg l^{-1} resazurin in the culture medium in some of the tubes; under all of the assay conditions tested, resazurin usually became colourless in the first 4–6 h of anoxic incubation. Separate tubes were run for each data point to avoid O_2 exposure during sampling. Anoxic biotransformation experiments used commercial glass vials with teflon-stoppered metallic screw caps (Sigma-Aldrich Co., St. Louis, MO, USA). These vials are designed for headspace gas chromatography (GC) and we took advantage of this setup because, similarly to the setup in Hungate tubes, anoxic conditions were rapidly established. Exponentially growing cells were resuspended at an OD_{600} of ca. 1 in fresh medium, vials were filled

Table 1
Bacterial strains and plasmids used in this study.

Bacterial strain or plasmid	Relevant characteristics[a]	Source or references
Escherichia coli		
DH5α	Cloning host; Φ80*lacZ*ΔM15 *recA1 endA1 gyrA96 thi-1 hsdR17*(r_K^- m_K^+) *supE44 relA1 deoR Δ(lacZYA-argF)U169*	Hanahan and Meselson (1983)
CC118λ*pir*	Cloning host; *araD139 Δ(ara-leu)7697 ΔlacX74 galE galK phoA20 thi-1 rpsE rpoB*(Rif^R) *argE*(Am) *recA1*, λ*pir* lysogen	Herrero et al. (1990)
HB101	Helper strain; F$^-$ λ$^-$ *mcrB mrr hsdS20*(r_B^- m_B^-) *recA13 leuB6 ara-14 Δ(proBA)2 lacY1 galK2 xyl-5 mtl-1 rpsL20*(Sm^R) *glnV44*	Boyer and Roulland-Dussoix (1969)
MG1655[b]	Wild-type strain; F$^-$ λ$^-$ *ilvG rfb-50 rph-1*	Blattner et al. (1997)
BW25113[b]	F$^-$ λ$^-$ *Δ(araD-araB)567 ΔlacZ4787(::rrnB-3) rph-1 Δ(rhaD-rhaB)568 hsdR514*	Baba et al. (2006)
JW2293-1[b]	Same as BW25113, but Δ*pta779::aphA*, Km^R	Baba et al. (2006)
Pseudomonas putida		
KT2440	Wild-type strain, spontaneous restriction-deficient derivative of strain mt-2 cured of the TOL plasmid pWW0	Bagdasarian et al. (1981)
KT2440 Δ*pta*	Same as KT2440, but Δ*pta*::mini-Tn*5*, Km^R	Duque et al. (2007)
Pseudomonas pavonaceae		
170	Wild-type strain, 1,3-dichloroprop-1-ene degrader isolated from contaminated soils	Verhagen et al. (1995)
Zymomonas mobilis		
DSM 424	Wild-type strain, produces ethanol under anoxic growth conditions	Deutsche Sammlung von Mikroorganismen und Zellkulturen GmbH; Braunschweig, Germany
Plasmid		
pRK600	Helper plasmid used in tri-parental matings; *oriV(ColE1)* RK2 *tra*$^+$ *mob*$^+$, Cm^R	Kessler et al. (1994)
pSEVA234[c]	Expression vector; *oriV*(pBBR1) *lacI*^{Q} P_{trc} *aphA*, Km^R	Silva-Rocha et al., in press
pSEVA428[c]	Expression vector; *oriV*(RK2) *xylS Pm aadA*, Sm^R	Silva-Rocha et al., in press

[a] Antibiotic markers: Cm, chloramphenicol; Km, kanamycin; Rif, rifampicin; Sm, streptomycin.
[b] Strains obtained from the *E. coli* Genetic Stock Center (Yale University, New Haven, CT, USA).
[c] Plasmids belonging to the SEVA (Standard European Vector Architecture) collection (Silva-Rocha et al., in press).

up to 75% of their nominal volume, and cells were exposed to 0.5 mM 1,3-DCP. The solubility of *cis*-1,3-DCP and *trans*-1,3-DCP in H_2O at 25 °C is 19.6 and 20.9 mM, respectively. The expression of relevant genes in the recombinants was induced during oxic growth to ensure proper biodegradation of organohalides and rapid metabolic adaptation when transferring the cells into anoxic conditions. Vials were incubated at 30 °C with rotary agitation to prevent biomass sedimentation, and one vial was used per time point for further analysis. Cells were immediately used in the biochemical assays or, for headspace GC coupled to mass spectrometry (MS) analysis, cells were rapidly inactivated by incubating the vials at 85 °C for 15 min. Vials were cooled to room temperature and stored at −20 °C until analysis.

Growth was estimated by measuring the OD_{600} after diluting the culture with 9 g l^{-1} NaCl to match the linear response of the spectrophotometer toward biomass. OD_{600} was assessed using an Ultrospec 3000 *pro* UV/Visible Spectrophotometer (GE Healthcare Bio-Sciences Corp., Piscataway, NJ, USA). All solid media used in this work contained 15 g l^{-1} agar, and the following antibiotics were added when appropriate as filter-sterilised solutions: kanamycin (50 μg ml^{-1}), chloramphenicol (30 μg ml^{-1}), and/or streptomycin (100 μg ml^{-1}). Isopropyl-β-D-thiogalactopyranoside (IPTG) was added at 1 mM to induce the expression of genes under the control of LacI^Q/P_{trc}, and 3-methylbenzoate (3-*m*B) was added at 2.5 mM to induce the expression of genes under the control of XylS/*Pm*.

2.2. Nucleic acid manipulation and general cloning techniques

DNA segments were amplified by PCR using 50–100 ng of the appropriate template, which was mixed in a 50-μl reaction mixture containing 20 mM Tris·HCl (pH=8.8), 10 mM KCl, 2 mM $MgSO_4$, 10 mM $(NH_4)_2SO_4$, 0.1% (w/v) Triton X-100, 0.1 mg ml^{-1} nuclease-free bovine serum albumin, 50 pmol of each primer, 200 μM of each dNTP, and 2.5 units of *Pfu* DNA polymerase (Promega, Madison, WI, USA). After an initial DNA denaturation step of 3 min at 94 °C, the reaction mixtures were subjected to 25–30 cycles consisting of 1 min at 94 °C, 30 s at 55 °C, and 2–4 min at 74 °C. Clones were checked by colony PCR using 1.25 units of *Taq* DNA polymerase (Promega). All of the primer oligonucleotides used in this study were purchased from Sigma-Aldrich Co., and their sequences are listed in Table S1 (Supplementary material). Restriction enzymes were obtained from New England Biolabs (Ipswich, MA, USA), and T4 DNA ligase was purchased from Roche Applied Science (Indianapolis, IN, USA). DNA fragments were purified from agarose gels using a purification kit from Macherey–Nagel GmbH & Co. KG (Düren, Germany). Genomic DNA was isolated from *Z. mobilis* as described by Byun et al. (1986), and from *P. pavonaceae* 170 and *E. coli* as detailed by Sambrook and Russell (2001), and stored at −20 °C until use. Plasmid inserts obtained by PCR were verified by DNA sequencing using the dideoxy chain termination method.

Plasmids were transferred into *P. putida* KT2440 and its derivatives using the filter mating procedure described in detail by de Lorenzo and Timmis (1994). Briefly, 0.22-μm filters containing the biomass resulting from a mixture of equal volumes of the donor strain, the recipient, and the helper strain (*E. coli* HB101 carrying pRK600) were incubated for 18 h at 30 °C on LB plates. Cells from the filter surface were then suspended in 10 mM $MgSO_4$, and appropriate dilutions were plated onto selective medium [M9 minimal medium supplemented with 0.2% (w/v) sodium citrate and the required antibiotics] to select *P. putida* exconjugants.

2.3. Cloning of *ackA* from *Escherichia coli* and *pdc-adhB* from *Zymomonas mobilis*

The acetate kinase (*ackA*) gene was amplified by PCR using genomic DNA from *E. coli* MG1655 as the template and oligonucleotides *ackA*^{Ec}-F and *ackA*^{Ec}-R. The 1242-bp fragment was cloned as an *Avr*II–*Eco*RI fragment into the multiple cloning site of the expression plasmid pSEVA234 (LacI^Q/P_{trc}). The pyruvate decarboxylase (*pdc*) and alcohol dehydrogenase II (*adhB*) genes were separately amplified by PCR using genomic DNA from *Z. mobilis* DSM424 as the template and oligonucleotides *pdc*^{Zm}-F and *pdc*^{Zm}-R or *adhB*^{Zm}-F and *adhB*^{Zm}-R, obtaining two fragments

of 1745 and 1208 bp, respectively. The second step consisted of sewing (cross-over) PCR (Horton et al., 1990) and generation of a synthetic operon using the amplification products from the first step as the template and primers pdc^{Zm}-F and $adhB^{Zm}$-R. The 2923-bp amplicon spanned the *pdc* and *adhB* genes as a single transcriptional unit flanked by recognition sites for *Sac*I and *Sph*I. This amplicon was digested with *Sac*I and *Sph*I and ligated into pSEVA234 and a derivative of this plasmid carrying $ackA^{E.\ coli}$ previously digested with the same restriction enzymes. In all of these constructs, a Shine–Dalgarno motif was included before the ATG codon of the corresponding gene, and the native stop codons were changed to TAA.

2.4. Construction of a fluorescent protein reporter for anaerobic cells

The blue-light photoreceptor YtvA from *Bacillus subtilis* was previously engineered to turn it into a reporter protein able to fluoresce in the absence of O_2 (Drepper et al., 2007). YtvA is a 261-amino acid protein consisting of two functional domains: the photoactive *N*-terminal light-O_2-voltage domain (amino acid residues 25–126) and the C-terminal sulphate transporter/anti-σ factor antagonist domain (amino acid residues 147–258), the latter carrying a nucleoside triphosphate-binding motif. The coding sequence for the first 137 amino acids in the *N*-terminal domain of YtvA was optimised for expression in *E. coli* by Drepper et al. (2007) and the resulting protein was termed EcFbFP, which stands for *E. coli*-optimised flavin mononucleotide-based fluorescent protein. EcFbFP emits strong fluorescence at 495 nm upon excitation with blue light (450 nm) (Drepper et al., 2007; 2010). A 445-bp DNA fragment spanning the entire EcFbFP coding sequence was obtained by PCR using oligonucleotides EcFbFP-F and EcFbFP-R, which introduce a Shine–Dalgarno motif before the ATG codon and eliminates a *Sma*I/*Xma*I site in the coding sequence to facilitate further cloning. This amplicon was inserted as a *Hin*dIII–*Spe*I fragment into the expression plasmid pSEVA428 (XylS/*Pm*).

2.5. Construction of a synthetic operon for the degradation of organohalides by recruiting genes from Pseudomonas pavonaceae 170

A synthetic operon, termed AHDO (alkyl halide degradation operon), was constructed by sewing (cross-over) PCR (Horton et al., 1990) as follows. A first fragment, comprising *dhaA*, was amplified using genomic DNA from *P. pavonaceae* 170 as the template and oligonucleotides *dhaA*-F and *dhaA*-R. The *caaD*1 and *caaD*2 genes were amplified as a single DNA fragment with oligonucleotides *caaD*1-F and *caaD*2-R. Finally, sewing PCR amplification was used to generate the synthetic operon using a mixture of the amplification products from the first and second steps as the template and the external oligonucleotides (i.e., *dhaA*-F and *caaD2*-R). The 1386-bp amplicon spanned the *dhaA*, *caaD*1, and *caaD*2 genes from *P. pavonaceae* 170 as a single transcriptional unit bracketed by *Kpn*I and *Hin*dIII restriction sites, and a Shine–Dalgarno motif was included before the ATG codon of the *dhaA* and *caaD*1 genes. This fragment was cloned into the expression plasmid pSEVA428 (XylS/*Pm*) digested with the same enzymes.

2.6. Preparation of cell-free extracts and in vitro determination of enzyme activities

Cell-free extracts were prepared from cells grown to mid-exponential phase (OD_{600} of 0.5–0.6) and harvested by centrifugation from an appropriate culture volume (10–35 ml) at 4000 × *g* at 4 °C for 10 min. Pellets were suspended in 1 volume of 10 mM sodium phosphate buffer (pH = 7.5, previously refrigerated) containing 0.1 M 2-mercaptoethanol and centrifuged again as described above. Cells were finally resuspended in 0.3–0.5 volume of the same buffer and sonicated intermittently for 6 min in an ice bath. A similar procedure was used to prepare cell-free extracts for haloalkane dehalogenase activity determinations, but the cells were washed and resuspended in 0.3–0.5 volume of a buffer composed of 10 mM Tris · H_2SO_4 (pH = 8.2), 1 mM EDTA, 1 mM 2-mercaptoethanol, 0.02% (w/v) NaN_3, and 10% (v/v) glycerol. In both cases, the sonicated cells were centrifuged at 7500 × *g* at 4 °C for 30 min to remove cell debris and to reduce the NADH/NAD^+ background in the lysate. Total protein concentration in cell extracts was measured by the Bradford method (Bradford, 1976) using a commercially available kit from Sigma-Aldrich Co., with crystalline bovine serum albumin as the standard.

Phosphotransacetylase (Pta) activity was determined spectrophotometrically at 30 °C by following the formation of acetyl-coenzyme A (CoA) from acetyl-phosphate and CoA that results in an increase of absorption at 233 nm (Hartmanis and Gatenbeck, 1984). The assay mixture (600 µl final volume) contained 90 mM Tris · HCl buffer (pH = 8.0), 90 mM KCl, 0.2 mM CoA, 14.5 mM acetyl-phosphate, and an appropriate volume of the cell-free extract. The addition of acetyl-phosphate initiated the reaction. An extinction coefficient (ε_{CoA}) of 4.44 $mM^{-1}\ cm^{-1}$, representing the difference between the extinction coefficients of acetyl-CoA and free CoA, was used in the Pta assay. One unit of activity was defined as the quantity of enzyme that catalysed the formation of 1 µmol of acetyl-CoA during 60 min at 30 °C. The acetate kinase activity assay is based on the formation of acetyl-hydroxamate (Brown et al., 1977). The assay mixture (1 ml final volume) contained 50 mM Tris · HCl (pH = 7.4), 10 mM $MgCl_2$, 10 mM ATP, 800 mM CH_3COOK, and 700 mM of freshly neutralised NH_2OH. The cell-free extract was added to the reaction mixture and incubated 5 min at room temperature (ca. 25 °C), after which 1 ml of 10% (w/v) trichloroacetic acid was added followed by 1 ml of freshly-prepared 1.25% (w/v) $FeCl_3$ in 1 N HCl. After another 5-min incubation period at room temperature, the mixture was centrifuged at maximal velocity during 1 min in a microfuge (Eppendorf centrifuge 5415D; Eppendorf North America, Inc., Hauppauge, NY, USA), and the absorbance of the supernatant was recorded at 540 nm. The colour was stable for at least 1 h, and a standard curve for acetyl-hydroxamate was prepared using lithium acetyl-phosphate as the acetyl donor. One unit of activity was defined as the quantity of enzyme that catalysed the formation of 1 µmol acetyl-hydroxamate in 5 min at 25 °C. Pyruvate decarboxylase (Pdc) catalyses the decarboxylation of pyruvate to acetaldehyde. The assay is an indirect method in which the conversion is linked to the activity of the subsequent enzyme alcohol dehydrogenase, that is supplied in excess and effectively converts acetaldehyde into NAD^+ and ethanol (Diefenbach and Duggleby, 1991). The assay mixture (1 ml final volume) contained 50 mM 2-(*N*-morpholino)ethanesulfonic acid · KOH (pH = 6.5), 5 mM $MgCl_2$, 0.1 mM thiamine diphosphate, 0.15 mM NADH, 10 units ml^{-1} alcohol dehydrogenase (from *Saccharomyces cerevisiae*, Sigma-Aldrich Co.), and 5 mM pyruvate. Alcohol dehydrogenase (AdhB) activity was assayed by measuring the ethanol-dependent reduction of NAD^+ (Hoppner and Doelle, 1983; Neale et al., 1986). The assay mixture (1 ml) contained 50 mM sodium phosphate buffer (pH = 6.5), 333 mM ethanol, and 8.3 mM NAD^+. In both Pdc and AdhB assays, the cell-free extract was added to the reaction mixture, and the rate of change of absorption at 340 nm was recorded at 30 °C. An extinction coefficient (ε_{NADH}) of 6.22 $mM^{-1}\ cm^{-1}$, representing the difference between the extinction coefficients of NADH and NAD^+, was used in both assays. One unit of activity was defined as the quantity of enzyme that catalysed the formation of 1 µmol product in 1 min at 30 °C.

Haloalkane dehalogenase assays were performed by incubating an appropriate amount of cell extract with 3 ml of a 5-mM substrate solution in 50 mM Tris·H_2SO_4 buffer (pH=8.2) at 30 °C (Janssen et al., 1987a; Poelarends et al., 1999). Halide liberation was monitored colourimetrically with the method described by Bergmann and Sanik (1957), which depends upon displacement of the thiocyanate ion from mercuric thiocyanate by inorganic chloride. In the presence of ferric ion, a highly coloured ferric thiocyanate complex is formed, according to the reaction $2Cl^- + Hg(SCN)_2 + 2Fe^{3+} \rightarrow HgCl_2 + 2Fe(SCN)^{2+}$. For routine determinations, 1-chlorobutane or 1,3-DCP was used as the substrate. Halide production (in the range 0 to 1 mM) was determined spectrophotometrically at 460 nm. One unit of activity was defined as the quantity of enzyme that catalysed the formation of 1 μmol of halide during 1 min at 30 °C. In each set of determinations, the dehalogenase activity in the samples was corrected for abiotic dehalogenation (which consistently accounted for $\leq$2.5% of the total activity) and the signal produced by the chloride ion present in buffers and reagents. Screening of dehalogenase activity in recombinants was carried out by incubating a small amount of the cell suspension to be tested in a microtiter plate with 150 μl of a mixture of 5 mM 1,3-DCP in 50 mM Tris·H_2SO_4 buffer (pH=8.2). After overnight incubation of the plate at 30 °C, 100 μl of 0.25 M $NH_4Fe(SO_4)_2$ in 6 M HNO_3 was added, followed by a drop of saturated $Hg(SCN)_2$ in ethanol.

2.7. Determination of the ATP/ADP ratio and the adenylate energy charge

Deproteinised cell extracts were prepared by promptly mixing 0.75 ml of the corresponding bacterial culture with a slurry composed by 0.75 ml phenol [equilibrated with 10 mM Tris and 1 mM EDTA (pH=8), and pre-heated at 80 °C] and 0.5 g glass beads (106 μm in diameter; Sigma-Aldrich Co.), followed by vigorous vortexing for 30 s. After standing 30 min at room temperature, samples were vortexed again for 30 s. Two phases were distinctly separated by centrifugation at 12500×*g* for 10 min at 4 °C in an Eppendorf microfuge, and the aqueous phase was subsequently treated twice with 1 volume of $CHCl_3$ to extract any residual phenol. These extracts were kept on ice and immediately used for adenine nucleotide assays. The adenylate energy charge (AEC) is a quantitative measure of the relative saturation of high-energy phosphoanhydride bonds available in the adenylate pool of the cell (Chapman et al., 1971; Lundin et al., 1986), and can be expressed according to the formula AEC=([ATP]+0.5[ADP])/([ATP]+[ADP]+[AMP]).

The first part of the assay comprised the irreversible conversion of ATP to AMP and PP_i with ATP sulfurylase in the presence of molybdate (Schultz et al., 1993). The reaction mixture consisted of 50 mM Tris·HCl (pH=8.0), 5 mM $MgCl_2$, 10 mM Na_2MoO_4, 2.5 mM GMP, an appropriate amount of deproteinised and neutralised sample (contributing to $\leq$25% of the total volume), and 0.5 units of adenosine-5′-triphosphate sulfurylase (from *S. cerevisiae*, Sigma-Aldrich Co.). Reactions were incubated at 30 °C for 20 min, after which adenosine-5′-triphosphate sulfurylase was inactivated for 10 min at 70 °C. Residual ATP was quantified in aliquots of the resulting extracts and consistently accounted for $\leq$2% of the original amount. In the second part of the assay, the ADP present in the samples was converted to ATP by mixing a 100-μl aliquot of the ATP sulfurylase-treated samples with 100 μl of a reaction mixture containing 45 mM Tris·HCl (pH=8.0), 4.5 mM $MgCl_2$, 36 mM KCl, 0.5 mM phosphoenolpyruvate, and 1.5 units of pyruvate kinase (from rabbit muscle, Sigma-Aldrich Co.) (Nilsson et al., 1996). Reactions were incubated at 25 °C for 30 min, after which 800 μl of milli-Q H_2O were added. ADP-derived ATP was assayed in these extracts. ADP was calculated as the difference between the ATP measured following incubation with pyruvate kinase and the residual ATP measured following treatment with ATP sulfurylase alone. For AMP determinations, 1.25 units of adenylate myokinase (from rabbit muscle, Sigma-Aldrich Co.) was also added to a separate assay. In addition to the AMP, ADP, and ATP standards used to run calibration curves, some of the experimental samples were spiked with known amounts of each nucleotide, and in all cases the results were corrected for quenching of the ATP signal by the presence of pyruvate kinase and/or adenylate myokinase.

2.8. Other analytical procedures

Flow cytometry analysis of EcFbFP fluorescence levels and quantification of propidium iodide exclusion were performed in a Gallios™ flow cytometer (Beckman Coulter Inc., Indianapolis, IN, USA) equipped with an argon ion laser of 15 mW at 488 nm as the excitation source and following well established protocols (Coder, 1997; Nikel and de Lorenzo, 2012). Fluorescence emission was detected using a 530/30-nm band pass filter set. Data for at least 10000 cells per experiment were collected, and the data were analysed using Cyflogic™ 1.2.1 software (CyFlo Ltd., Turku, Finland).

Headspace GC–MS analysis of 1,3-DCP was performed with a Varian3000 gas chromatograph and a 4000MS ion trap mass spectrometer (Bruker Daltonik GmbH, Bremen, Germany) equipped with a Combi PAL™ auto sampler (Altmann Analytik GmbH & Co. KG, Munich, Germany). Sample volumes of 100 μl were injected at 250 °C (injector temperature) without split. A 30 m×0.25 mm×0.25 μm FactorFour™ 5 ms column (low polarity phase, 5% phenyl and 95% dimethylpolysiloxane, Bruker Daltonik GmbH) was used, and the interface and ion source temperature were adjusted to 230 °C and 200 °C, respectively. The He carrier gas was set to a constant flow of 0.6 ml min^{-1}. After 6 min of constant heating at 35 °C, the oven temperature was raised in a temperature ramp of 10 °C min^{-1} to 250 °C. To equilibrate the system for the next injection, the temperature was set to 35 °C for 10 min. Mass spectra were recorded at 2 scans s^{-1} with a scanning range of m/z=50–301. Evaluation of the chromatograms was performed with the Varian Star Workstation™ 6.2 software (Bruker Daltonik GmbH). Metabolites were identified by comparing to the NIST Atomic Spectra Database version 4 (National Institute of Standards and Technology, Gaithersburg, MD, USA) and purified standards. Automatic peak quantification of the selected metabolites was implemented in the processing setup of the Varian Star Workstation™ 6.2 software. Virtual fragmentations were also performed separately with the Mass Frontier™ 2.0 software (Thermo Fisher Scientific Inc.). Acetate and ethanol concentrations in culture supernatants were determined using enzymatic kits (R-Biopharm AG, Darmstadt, Germany) as per the manufacturer's instructions.

2.9. Statistical analysis

All of the reported experiments were independently repeated at least twice (as indicated in the corresponding figure legend), and the mean value of the corresponding parameter ± standard deviation is presented. The level of significance of the differences when comparing results was evaluated by means of analysis of variance (ANOVA), with α=0.01 and 0.05.

3. Results and discussion

3.1. Pseudomonas putida KT2440 as a chassis for anoxic biotransformations: Comparison with related bacterial species and functional analysis of its extant genetic capabilities

It has been postulated that the central metabolism in *P. putida* is geared for the aerobic oxidation of hexoses, such as D-glucose

(Fuhrer et al., 2005). Specifically, this carbon source is first converted into pyruvate and D-glyceraldehyde-3-*P* through the Entner–Doudoroff pathway, pyruvate is later transformed into acetyl-CoA by the pyruvate dehydrogenase complex, and this metabolite is finally oxidised in the tricarboxylic acid cycle (Fig. 1; Blank et al., 2008; Chavarría et al., 2012). Reducing equivalents generated in these pathways (i.e., NADH) are used as electron donors for the respiratory chain, which ultimately leads to ATP synthesis. Thus, pseudomonads, microorganisms that rely on oxic respiration for growth under most environmental conditions, accumulate an excess of NADH when O_2 (or alternative terminal electron acceptors in some *Pseudomonas* species) becomes limiting. However, some pseudomonads, such as the ubiquitously-distributed opportunistic pathogen *Pseudomonas aeruginosa*, can rely on pyruvate fermentation for survival under conditions with restricted O_2 supply, thereby generating a mixture of D-lactate, acetate, and succinate as the main by-products during the breakdown of hexoses (Eschbach et al., 2004). *P. aeruginosa* also grows under anoxic conditions in the presence of NO_3^- or NO_2^- *via* denitrification (Arai, 2011; Shiro et al., 2012). *Pseudomonas mendocina* produces a mixture of D-lactate, acetate, formate, ethanol, and uronic acids when grown in D-glucose—limited anoxic chemostat cultures (Verdoni et al., 1992). In stark contrast, an *in silico* genome-wide analysis of the metabolic capabilities of *P. putida* KT2440 revealed that anoxic catabolism of hexoses in this microorganism is most likely hampered by the lack of *bona fide* fermentation pathways or a suitable anoxic electron transport chain.

Attempts to grow *P. putida* KT2440 under anoxic conditions in our laboratory, even in the presence of alternative electron acceptors such as NO_3^-, completely failed (data not shown). We first considered that the absence of anoxic growth could be due to a shortage of building blocks needed for biomass synthesis related to the strong reduction in the activity of the pyruvate dehydrogenase complex when O_2 becomes limiting (and, consequently, the NADH/NAD^+ ratio is expected to increase). In *E. coli*, the radical enzyme pyruvate-formate lyase converts pyruvate into acetyl-CoA and formate under anoxic conditions, thus providing carbon skeletons for the lower metabolic pathways when the pyruvate dehydrogenase complex no longer catalyses the conversion of pyruvate (Sawers and Böck, 1988). With this idea in mind, we first aimed to introduce a pyruvate-formate lyase activity into *P. putida* by heterologous expression of the *pflAB* genes from *E. coli*, but this strategy proved unsuccessful as no PflB activity was detected in cell-free extracts of *P. putida* recombinants incubated under restricted O_2 supply (data not shown). In its native context, PflB requires the activity of at least one activator protein (PflA, but also TdcE and/or YfiD) and an unstable organic free radical in the polypeptide, only formed under strict anoxic conditions (Knappe and Sawers, 1990). It is possible that under the conditions tested in this study, PflB failed to be activated by the cognate PflA protein, and/or that the glycyl radical in PflB was not formed at all. We therefore focused on metabolic manipulations that could result in a significant alteration of the energy and redox state of the cells while leaving intact the native pathways for pyruvate processing.

By examining the genome database and the currently available metabolic models of *P. putida* KT2440 (Nogales et al., 2008; Puchalka et al., 2008; Sohn et al., 2010), we found several genes that might be involved in anoxic pathways (see Table S2 in the Supplementary material). These genes fall into two main categories. Alternative respiratory processes are represented by two subunits of a nitrite reductase and at least three genes with nitroreductase capabilities. On the other hand, possible fermentation pathways include two lactate dehydrogenases, at least one formate dehydrogenase, and a number of alcohol and aldehyde dehydrogenases with reportedly different substrate specificities and co-factor requirements. However, no significant levels of D-lactate, formate, or ethanol could be enzymatically detected in supernatants of *P. putida* KT2440 suspensions anoxically incubated during 24 h (details not shown), suggesting that the activity through these (putative) fermentation pathways is rather low or even absent, and that they do not endow the cells with a true anoxic metabolism based on fermentation of D-glucose.

Interestingly, the genome of *P. putida* KT2440 also encodes an incomplete pathway for acetate synthesis from acetyl-CoA. In Enterobacteria and in *P. aeruginosa* this pathway is composed of a phosphate acetyltransferase (phosphotransacetylase) and an acetate kinase, and the genes encoding these activities often form an operon (Dittrich et al., 2005; Eschbach et al., 2004). *P. putida* KT2440 only encodes a *pta* (PP0774, annotated as phosphate acetyltransferase; Fig. 2A) and completely lacks an acetate kinase gene. Whereas the $pta^{P.\ putida}$ coding sequence predicts a 74.6-kDa protein, $pta^{E.\ coli}$ and $pta^{P.\ aeruginosa}$ encode 77.2 and 75.7 kDa polypeptides, respectively. The acetate metabolic pathway in the genome of *P. putida* is also represented by at least three acetate transporters (belonging to the *actP* permease family) encoded by PP1743, PP2797, and PP3272. Prompted by this surprising asymmetry in the genetic organisation surrounding $Pta^{P.\ putida}$ when compared to the homologous pathway in Enterobacteria and *P. aeruginosa*, we next studied whether any Pta activity is present in *P. putida* KT2440.

3.2. The energy state of Pseudomonas putida KT2440 under anoxic conditions is altered by the heterologous expression of an acetate kinase from Escherichia coli

To verify the functionality of *pta* in *P. putida* KT2440, we quantified the specific phosphotransacetylase activity in cell-free extracts of the wild-type strain during growth in M9 minimal

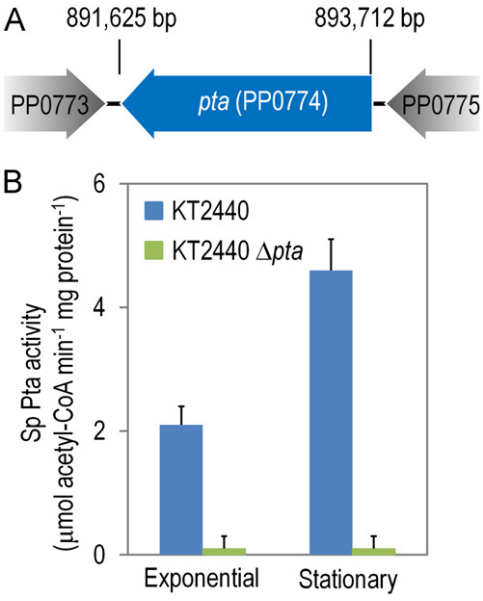

Fig. 2. Genetic and biochemical characterisation of phosphotransacetylase (Pta) in *P. putida* KT2440. (A) Genetic organisation of the *pta* locus. The *pta* gene (PP0774) is flanked upstream by PP0773, which encodes an OmpA/MotB domain protein, and downstream by PP0775, which encodes an uncharacterised hypothetical protein. (B) *In vitro* evaluation of the specific (Sp) Pta activity in cell-free extracts of *P. putida* KT2440 and its Δ*pta*::mini-Tn*5* mutant derivative grown in oxic batch cultures in M9 minimal medium containing 10 g l^{-1} D-glucose as the sole carbon source. Bars represent the mean value of the specific enzymatic activity ± standard deviation of triplicate measurements from at least two independent experiments.

medium containing D-glucose as the sole carbon source (Fig. 2B). We detected a 2.2-fold increase in Pta activity when the cells transitioned from logarithmic growth into the stationary phase, perhaps as a consequence of acetyl-CoA accumulation during active growth, followed by a marked reduction in the activity of the pyruvate dehydrogenase complex as expected by the decrease in O_2 availability. In a parallel experiment using a *P. putida* KT2440 mutant in which *pta* was interrupted with a mini-Tn*5* transposon (Duque et al., 2007), we did not detect any significant activity, suggesting that the enzymatic activity was dependent on an intact *pta* gene. These results suggest that Pta is indeed active in *P. putida* KT2440 in a growth-phase dependent fashion, but its relevance (if any) on the cell physiology remains uncertain. The level of Pta activity in *P. putida* was significantly lower than that observed in *E. coli* BW25113 grown in the same culture conditions, which peaked at 12.5 ± 0.9 units mg protein^{-1} at the onset of the stationary phase. The activity of the Pta-AckA pathway in Enterobacteria is coupled to acetate synthesis in both oxic and anoxic growth conditions (Brown et al., 1977; Dittrich et al., 2005), and it is known to regulate the intracellular acetyl-CoA availability. In fact, a Δ*pta*::*aphA* derivative of *E. coli* BW25113 showed impaired growth in M9 minimal medium containing D-glucose during oxic growth, resulting in a 2.3-fold lower specific growth rate and in a 1.6-fold reduction in the final biomass concentration when compared to the parental strain ($P < 0.01$, ANOVA).

When D-glucose is processed through the Entner–Doudoroff pathway it generates 1 mol ATP mol D-glucose^{-1}, an energy yield lower than that obtained through the activity of the Embden–Meyerhof–Parnas pathway (Conway, 1992). Because *P. putida* KT2440 uses the Entner–Doudoroff pathway for D-glucose catabolism, we hypothesised that in the absence of biochemical reactions for oxidative phosphorylation (i.e., respiratory processes), ATP generation *via* substrate-level phosphorylation could be an alternative to fulfil anoxic energy requirements. We next evaluated whether acetyl-phosphate stemming from the Pta$^{P.\ putida}$ activity could be used as a substrate for a heterologous, ATP-producing acetate kinase (Fig. 3A). To test this hypothesis, the native Pta activity in *P. putida* KT2440 was functionally complemented by adding the AckA enzyme (annotated as acetate kinase A and propionate kinase 2, E.C. 2.7.2.1; Keseler et al., 2011) from the facultative anaerobic enterobacteriaceae *E. coli*. To this end, *ackA* from *E. coli* MG1655 was amplified by PCR and placed under the control of the inducible P_{trc} promoter in the medium-copy-number expression vector pSEVA234. Upon the induction of *ackA* expression by IPTG, we observed a sharp increase in the acetate kinase activity in cells incubated under anoxic conditions, which went up to 17.8 ± 1.3 units mg protein^{-1} (Fig. 3B). Moreover, under these conditions, the recombinant strain produced (and secreted) up to 12.9 ± 0.6 mM acetate, whereas in control experiments (i.e., *P. putida* KT2440 carrying pSEVA234), the acetate levels in culture supernatants consistently remained below 1 mM. The expression of *ackA*$^{E.coli}$ in a *pta*::mini-Tn*5* background resulted in acetate secretion to levels similar to those found in the wild-type strain carrying the empty vector, thus confirming that acetate synthesis in the recombinant *P. putida* strain uses acetyl-phosphate from the native Pta reaction as the precursor metabolite.

We next evaluated whether the activity of the Pta-AckA pathway influences the energy charge of *P. putida*. Measuring the ATP/ADP ratio served as a coarse estimation of the energy state in the cells. Cell suspensions were incubated for 24 h under anoxic conditions, and the content of adenine nucleotides was enzymatically determined as detailed in Section 2. Under these conditions, the ATP/ADP ratio in the recombinant strain bearing AckA$^{E.\ coli}$ was 6.2 ± 0.8 mol mol^{-1}, which represents a 1.3-fold

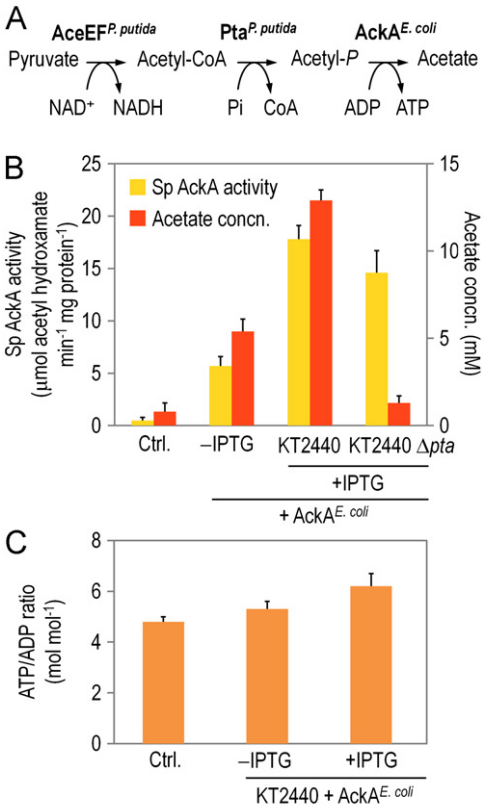

Fig. 3. Functional complementation of the phosphotransacetylase (Pta)-acetate kinase (AckA) pathway in *P. putida* KT2440 by introduction of AckA$^{E.\ coli}$. (A) The native Pta enzyme catalyses the phosphorylation of acetyl-coenzyme A (CoA), formed by the native pyruvate dehydrogenase complex, thereby generating acetyl-phosphate (acetyl-*P*) and free CoA. Acetyl-*P* was used as the substrate for the heterologous AckA bioreaction transplanted from *E. coli* MG1655, which produces acetate with the concomitant generation of ATP by a substrate-level phosphorylation reaction. (B) *In vitro* evaluation of the specific (Sp) AckA activity in cell-free extracts of *P. putida* KT2440 and its Δ*pta*::mini-Tn*5* mutant derivative grown in oxic batch cultures in M9 minimal medium containing 10 g l^{-1} D-glucose as the sole carbon source and subjected to anoxic conditions for 24 h after the addition of 1 mM IPTG to the culture medium to induce P_{trc}::*ackA*$^{E.\ coli}$ expression (see Section 2 for further experimental details). The acetate concentration (concn.) in culture medium supernatants was determined using an enzymatic kit. (C) Determination of the ATP/ADP molar ratios as an estimation of the energy state of the cells. Adenine nucleotide content was enzymatically measured after 24 h of anoxic incubation upon the induction of P_{trc}::*ackA*$^{E.\ coli}$ expression. In all cases, control experiments (Ctrl.) were conducted using *P. putida* KT2440 carrying the empty vector. Bars represent the mean value of the corresponding parameter ± standard deviation of triplicate measurements from at least two independent experiments.

increase in this parameter when compared to that observed in wild-type KT2440 carrying the empty vector under the same conditions ($P < 0.05$, ANOVA). This result proved interesting, showing that the distribution of adenine nucleotides changes upon the expression of *ackA*$^{E.\ coli}$. We decided to further characterise the energy state of the recombinant *P. putida* strains. Although the ATP/ADP ratio represents a useful estimation of the energy state, the AEC is a more accurate descriptor of the actual energy charge in the cells because it takes into account the intracellular concentration of all three phosphorylated forms of adenine (Chapman et al., 1971). Under oxic growth conditions, the AEC of *P. putida* KT2440 cells grown on D-glucose reached its maximum value (0.91 ± 0.12 mol mol^{-1}) during mid-exponential phase, i.e., when the specific growth rate also peaked at its maximum value. Correspondingly, an AEC value close to one reflects a high ATP content in the cells over ADP and AMP, which

is a metabolic trait characteristic of healthy cells during unrestricted growth.

Consistent with our hypotheses, the AEC values significantly dropped upon exposure of the cells to a low O_2 environment, most likely reflecting a reduction in the activity of the respiratory chain when O_2 becomes limiting (which in turn determines a low activity of the H^+-pumping F_0–F_1 ATP synthase). In fact, after 24 h of anoxic incubation, the AEC decreased to 0.28 ± 0.04 mol mol^{-1}. This rather low value is within the range reported in the literature for environmental conditions in which cell viability starts to be compromised (Chapman et al., 1971; Lundin et al., 1986). It has been suggested that the growth of *E. coli* can occur only at AEC values above ca. 0.8, cell viability is maintained at AEC values between 0.8 and 0.5, and cells start to die at AEC values < 0.5 (Andersen and von Meyenburg, 1977). In contrast to the behaviour of wild-type *P. putida* KT2440 carrying the empty vector, the AEC value in the strain bearing AckA$^{E.\ coli}$ initially dropped slightly but did not change significantly over a 24-h anoxic incubation period, remaining at ca. 0.62–0.69 mol mol^{-1} throughout. In all cases, the most dramatic changes were observed in the cellular ATP content and, to a lesser extent, in the cellular ADP content (as reflected in the ratio between these two phosphorylated forms of adenine), whereas the AMP concentration remained approximately the same among the different strains and culture conditions assayed. A similar behaviour regarding the qualitative distribution of adenine nucleotides was also observed by Neumann et al. (2006) when studying the physiological responses of the solvent-tolerant *P. putida* strain DOT-T1E when the cells were exposed to a second phase of 1-decanol. Considering that the sum of the three phosphorylated forms of the nucleotide was nearly constant but that the ATP concentration decreased as the bacterial growth progressed, the authors suggested that ADP and AMP were formed at the expense of ATP.

Even though the energy state of the cells, as judged by both the ATP/ADP ratio and the AEC value, was significantly higher in the recombinant strain carrying AckA$^{E.\ coli}$ as compared to the wild-type strain, this metabolic manipulation did not enable significant growth in the absence of O_2. Our efforts to improve this situation next lead us to try changing the redox metabolism of the cells instead of merely influencing the energy status of the bacteria of interest.

3.3. *The redox state of Pseudomonas putida KT2440 under anoxic conditions can be manipulated towards a more oxidised environment by the heterologous expression of the ethanol-synthesis pathway from Zymomonas mobilis*

The NADH and NAD^+ redox couple plays a major role in central metabolism, and the ratio of the reduced to the oxidised form is thought to be representative of the intracellular redox state (de Graef et al., 1999). Under oxic growth conditions, NADH is oxidised through the respiratory chain to generate ATP. In contrast, reducing equivalents from carbon catabolism can no longer be oxidised under anoxic conditions, and the intracellular NAD(P)H build-up is a metabolic signal that contributes to the shift of bacterial physiology into non-growing conditions. A paradigmatic example is that of *E. coli*, in which a high NADH/NAD^+ ratio is one of the signals that determines the transition from an oxidative metabolic regime towards mixed fermentation (Clark, 1989). Therefore, a high NADH/NAD^+ ratio might interfere with bacterial growth if the cells cannot adequately get rid of the excess nicotinamide dinucleotides in their reduced form when the respiratory chain has a low activity level.

With this background information in mind, we wondered if the impaired anoxic breakdown of hexoses in *P. putida* KT2440 could be due to the lack of an effective way to re-oxidise the reducing equivalents produced during the catabolism of D-glucose. To test this hypothesis, a heterologous pathway for ethanol synthesis from pyruvate was constructed by recruiting genes from the aerotolerant sphingomonadaceae *Z. mobilis* (Hayashi et al., 2012). This pathway comprises a pyruvate decarboxylase (annotated as thiamine pyrophosphate protein binding domain-containing protein, Kanehisa et al., 2012, ZMO1360; E.C. 4.1.1.1) that converts pyruvate into acetaldehyde, followed by the action of alcohol dehydrogenase II (AdhB, annotated as Fe-containing alcohol dehydrogenase, Kanehisa et al., 2012, ZMO1596; E.C. 1.1.1.1) that reduces acetaldehyde into ethanol with the concomitant oxidation of NADH into NAD^+ (Fig. 4 A). The *pet* operon that includes the metabolic activities described above has been cloned and expressed in a wide variety of bacteria, with ethanol production as the main objective (Bothast et al., 1999; Geddes et al., 2011). In fact, the expression of *pdc* and *adhB* in *E. coli* leads to ethanol concentration levels > 50 g l^{-1} from different carbon sources (Ohta et al., 1991). However, to the best of our knowledge, such an anaerobic pathway has not been introduced into a *Pseudomonas* species. Pdc$^{Z.\ mobilis}$ has been shown to exhibit a K_m value for pyruvate much lower than that of the pyruvate

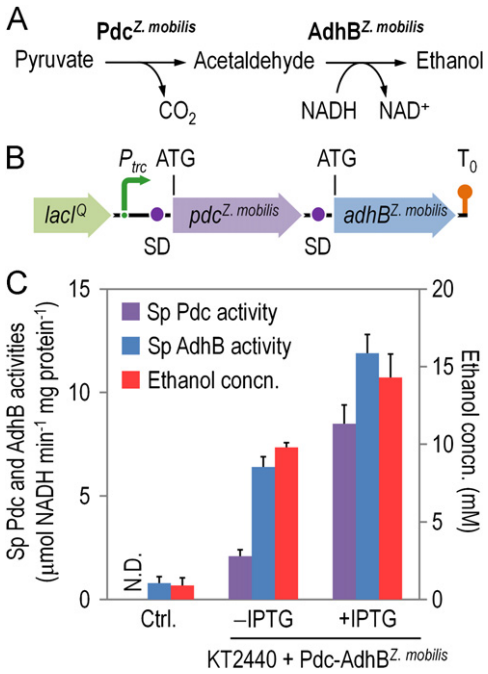

Fig. 4. Introduction of an ethanol synthesis pathway in *P. putida* KT2440 composed of enzymes recruited from *Z. mobilis*. (A) Pyruvate, generated from D-glucose through the activity of the Entner–Doudoroff pathway, is decarboxylated to acetaldehyde by pyruvate decarboxylase (Pdc$^{Z.\ mobilis}$, ZMO1360). Acetaldehyde is converted into ethanol by means of alcohol dehydrogenase II (AdhB$^{Z.\ mobilis}$, ZMO1596), together with the concomitant oxidation of one NADH molecule. Therefore, besides enabling ethanol synthesis, the activity of this pathway also influences the NADH/NAD^+ ratio in the cells. (B) Schematic representation of the synthetic operon in which *pdc*$^{Z.\ mobilis}$ and *adhB*$^{Z.\ mobilis}$ are placed under the control of an inducible LacI^Q/P_{trc} element as a single transcriptional unit. Each coding sequence was preceded with a Shine–Dalgarno (SD) motif, and the stop codons were edited to TAA. The transcriptional terminator of the bacteriophage λ is depicted as T_0. The elements in this outline are not drawn to scale. (C) *In vitro* evaluation of the specific (Sp) Pdc and AdhB activities in cell-free extracts of *P. putida* KT2440 grown in oxic batch cultures in M9 minimal medium containing 10 g l^{-1} D-glucose as the sole carbon source and subjected to anoxic conditions for 24 h after the addition of 1 mM IPTG to the culture medium to induce P_{trc}::*pdc-adhB*$^{Z.\ mobilis}$ expression (see Section 2 for further experimental details). The ethanol concentration (concn.) in culture medium supernatants was determined using an enzymatic kit. In all cases, control experiments (Ctrl.) were conducted using *P. putida* KT2440 carrying the empty vector. Bars represent the mean value of the corresponding parameter $\pm$ standard deviation of triplicate measurements from at least three independent experiments. N.D., not detected.

dehydrogenase complex of *E. coli* (Bringer-Meyer et al., 1986; Diefenbach and Duggleby, 1991), which results in an efficient re-routing of this substrate into ethanol synthesis.

We constructed a synthetic operon by cloning the *pdc* and *adhB* genes from *Z. mobilis* DSM 424 as a single transcriptional unit and under control of the inducible P_{trc} promoter by sewing (cross-over) PCR (Fig. 4B). The resulting plasmid was transformed into *P. putida* KT2440, and the behaviour of the recombinants was analysed under anoxic conditions. Interestingly, the expression of $Pdc^{Z.mobilis}$ and $AdhB^{Z.mobilis}$ in *P. putida* KT2440 resulted in ethanol synthesis from D-glucose even under oxic conditions (data not shown). However, a more significant level of ethanol synthesis was observed in 24-h cell suspensions incubated under anoxic conditions. Both anaerobic enzymes were properly expressed in *P. putida* as judged by the levels of specific Pdc and AdhB activity in cell-free extracts of the recombinant strain (Fig. 4C). Interestingly, we observed significant activity of the heterologous enzymes even in the absence of IPTG induction. However, these activities increased significantly upon addition of 1 mM IPTG (4.1- and 1.9-fold for Pdc and AdhB, respectively; $P < 0.01$, ANOVA). In addition, a low (but clearly discernible) level of alcohol dehydrogenase activity was detected in the wild-type strain carrying the empty vector. This background activity can most likely be accounted for by any of the 24 alcohol dehydrogenases annotated in the *P. putida* KT2440 genome database (Table S2 in the Supplementary material). A similar behaviour as that of the enzyme activities was also observed in ethanol synthesis; in non-induced cultures of the recombinant strain, the concentration of ethanol reached 9.8 ± 0.3 mM, and this value shifted to 14.3 ± 1.5 mM when the cultures were supplemented with IPTG.

The activity of Pdc and AdhB and the levels of ethanol formation pointed to a fully functional expression of the ethanol synthesis pathway from *Z. mobilis* in *P. putida*. However, and as already observed in the strain expressing $ackA^{E.\ coli}$, the recombinant *P. putida* strain carrying the ethanol synthesis pathway failed to generate biomass under anoxic conditions.

3.4. Perturbation of the energy state and redox balance in *Pseudomonas putida* KT2440 results in enhanced bacterial survival under anoxic conditions

Because the individual expression of $ackA^{E.\ coli}$ or $pdc\text{-}adhB^{Z.\ mobilis}$ in *P. putida* was not sufficient to enable anoxic growth of the recombinants (although it certainly modified key metabolic aspects of the bacterial physiology), we assayed the effects of co-expressing both heterologous pathways on cell viability in anoxic cultures (Fig. 5). The activities of all of the heterologous enzymes added to *P. putida* KT2440 were measured in the recombinant strain. After 24 h of anoxic incubation, the specific activity of AckA was 7.4 ± 0.9 units mg protein^{-1}, and the specific activities of Pdc and AdhB reached 8.6 ± 0.4 and 19.3 ± 2.3 units mg protein^{-1}, respectively. These *in vitro* determinations of enzymatic activity in induced cultures ensured the proper expression of the relevant genes. As expected, the anoxic incubation of *P. putida* KT2440 resulted in a dramatic drop in cell viability during the first 24 h (Fig. 5A). In the control experiment (conducted with the wild-type strain transformed with the empty vector), cell viability decreased by ca. 1.8-fold, whereas in the three *P. putida* recombinant strains (i.e., bearing $AckA^{E.\ coli}$ and/or $Pdc\text{-}AdhB^{Z.\ mobilis}$), this parameter remained within the 93–96% range. The cell viability in all of the experimental strains trended downwards after 24 h, but the slope for the recombinants was softer than that observed for the wild-type strain. At the same time, a graded effect on cell viability was observed among the recombinants carrying each heterologous pathway separately and the recombinant expressing both $ackA^{E.\ coli}$ and $pdc\text{-}adhB^{Z.\ mobilis}$.

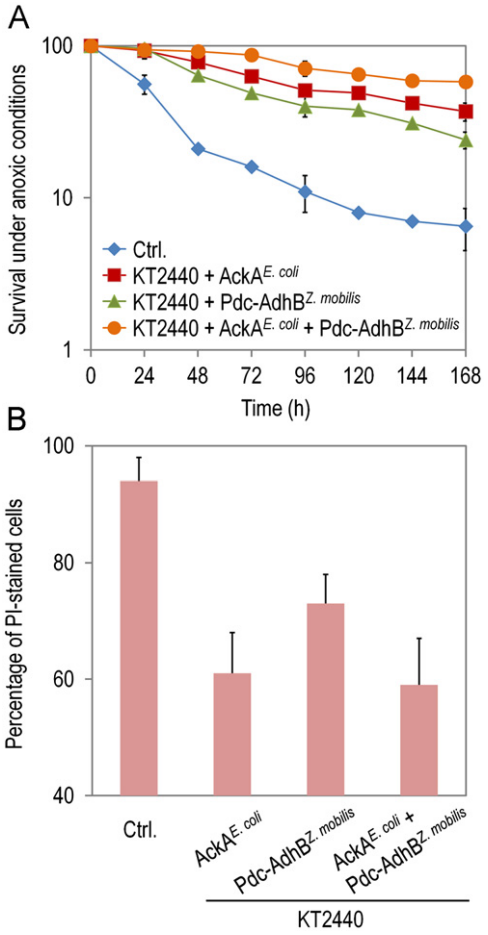

Fig. 5. Evaluation of survival and viability of the recombinants under anoxic conditions. (A) The ability of the recombinants to form colonies when transferred to fresh medium was evaluated after the indicated times of anoxic incubation by plating appropriate dilutions of the cell suspension onto LB plates. (B) Propidium iodide (PI) exclusion was used as a parameter to estimate cell viability. Appropriate dilutions of the cell suspension anoxically incubated for 168 h were stained with PI, and the percentage of PI-positive cells was determined by flow cytometry as detailed in Materials and methods. In all cases, control experiments (Ctrl.) were conducted using *P. putida* KT2440 carrying the empty vector(s). Each data point or bar represents the mean value of the corresponding parameter ± standard deviation of duplicate measurements from at least three independent experiments.

In fact, the latter strain was able to maintain a viability of $58 \pm 4\%$ after 168 h of anoxic incubation, compared to $37 \pm 3\%$ and $24 \pm 5\%$ for the $AckA^{E.\ coli}$ and the $Pdc\text{-}AdhB^{Z.\ mobilis}$ strains, respectively. After the same period of time, *P. putida* KT2440 carrying the empty vector had a viability of $7 \pm 4\%$. These results confirm that the alteration of the energy state and the intracellular redox balance have a deep impact on the cell physiology that resulted in altered (and enhanced) levels of viability under anoxic conditions, with values between 3.7- and 8.9-fold higher than that of the wild-type strain ($P < 0.01$, ANOVA). In particular, and by looking at the final cell viability values, it appears that an enhanced energy charge of the cells has a greater impact on the anoxic survival capability of the recombinants than that determined by altering the redox balance. These results are consistent with the predictions of the metabolic model of Sohn et al. (2010). The authors postulated that both the energy charge and viability of *P. putida* cells growing on glycerol or D-glucose as the carbon source could be enhanced by introducing a heterologous kinase activity for ATP synthesis. Moreover, these metabolic alterations seem to have an interesting synergistic effect that can be exploited to engineer a *P. putida* strain with extended survival

under anoxic conditions. The conversion of pyruvate into acetyl-CoA (needed as a substrate to support ATP generation by Pta$^{P.\ putida}$-AckA$^{E.\ coli}$) through the native pyruvate dehydrogenase complex (AceEF) is coupled to NADH formation (Fig. 3A). As NAD^+ recycling through the activity of Pdc-AdhB$^{Z.\ mobilis}$ fulfils redox homeostasis under anoxic conditions, this relationship between energy and redox balances can explain the observed synergistic effect between acetate production and ethanol fermentation in the recombinant strain carrying both heterologous pathways.

To further examine the metabolic vigour of the recombinant strains, we studied propidium iodide exclusion by cells anoxically incubated for 168 h by flow cytometry. Dye exclusion methods are based on the fact that only intact membranes are impermeable to large or charged molecules (Coder, 1997). Intact membranes also maintain cytoplasmic gradients with respect to the surrounding medium, thus retaining intracellular concentrations of ions and small molecules. Cells stained with propidium iodide are likely to be dead (or otherwise metabolically impaired), and the percentage of cells negative for the probe serves as a coarse estimation of viability and cell fitness. Whereas $94 \pm 5\%$ of the wild-type *P. putida* cells (carrying the empty pSEVA234 vector) were positive for propidium iodide, the fluorescence values for the recombinant strains were significantly lower (1.5-fold for the strain carrying AckA$^{E.\ coli}$, 1.3-fold for the strain carrying Pdc-AdhB$^{Z.\ mobilis}$, and 1.6-fold for the double-recombinant strain; Fig. 5B). These results qualitatively confirmed the trend observed for cell viability as measured by the ability of the experimental strains to form colonies when transferred into fresh medium. However, it is worth to mention that the percentage of metabolically fit cells as determined by PI staining and the population of actually viable cells may well differ as not all the cells promptly transferred from anoxic cultures to fresh medium retain their ability to form colonies under oxic conditions.

3.5. *Pseudomonas putida KT2440 carrying AckA$^{E.\ coli}$ and Pdc-AdhB$^{Z.\ mobilis}$ supports the activity of an anaerobic fluorescent protein*

The results obtained during the characterisation of the recombinants under anoxic conditions demonstrated that cell viability is enhanced by changes in the bacterial energy and redox statuses. However, *P. putida* KT2440 still failed to grow under such conditions. Therefore, the next pertinent question to be addressed was whether cells maintained a vigorous metabolic state even if it was not associated to significant growth. To clarify this, we used the reporter system based on the O_2-independent protein EcFbFP, originally derived from the *B. subtilis* blue-light receptor (Fig. 6A), the function of which requires active recycling of flavin mononucleotides (Drepper et al., 2007). The reporter plasmid, in which the transcription of the EcFbFP coding sequence is under the control of the XylS/*Pm* expression system, was introduced into *P. putida* KT2440 carrying the empty pSEVA234 vector and its derivative containing both AckA$^{E.\ coli}$ and Pdc-AdhB$^{Z.\ mobilis}$, and the fluorescence of EcFbFP was quantified in cells from oxic cultures and after 24 h of anoxic incubation upon induction with 3-*m*B. Although the fluorescence emitted by EcFbFP in both oxic and anoxic conditions in the recombinant strain was slightly lower than that observed in oxic cultures of the wild-type strain, the shift from oxic to anoxic conditions clearly did not affect the performance of the EcFbFP-based reporter. Whereas in the control strain the level of EcFbFP-mediated fluorescence dropped 4.8-fold when the cells were incubated in the absence of O_2, the fluorescence emitted by the recombinant strain did not change significantly (Fig. 6B), indicating that EcFbFP is active within this new metabolic milieu. This means that the energy-demanding transcriptional machinery required for the activity of *Pm* and the flavin mononucleotide redox cycle needed for EcFbFP fluorescence were present in the recombinant strain when deprived from O_2. Another physiological aspect that could influence the observed fluorescence levels is the translational activity of the cells under different O_2 availability regimes. However, considering that this trait is not expected to be significantly affected by the heterologous expression of the genes at stake in this study, it can be safely assumed that the differences in fluorescence levels are related to the modifications in the energy and redox homeostasis within the cells.

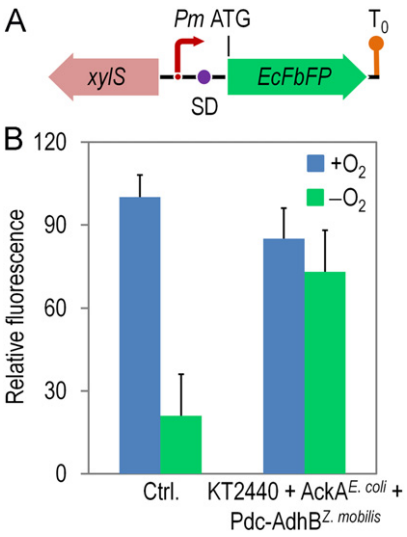

Fig. 6. Flow cytometry analysis of the expression of a reporter tailored for anaerobic cells. (A) Schematic representation of the reporter in which EcFbFP, a fluorescent protein derived from the blue-light photoreceptor YtvA from *B. subtilis*, is placed under the control of an inducible XylS/*Pm* element. The EcFbFP coding sequence was preceded with a Shine–Dalgarno (SD) motif, and the transcriptional terminator of the bacteriophage λ is depicted as T_0. The elements in this outline are not drawn to scale. (B) The ability of *P. putida* KT2440 recombinants to host the EcFbFP reporter was evaluated in both aerobic ($+O_2$) and anaerobic ($-O_2$) cells. In oxic cultures, cells were grown in M9 minimal medium containing 10 g l^{-1} D-glucose with 2.5 mM 3-*m*B as an inducer, and the fluorescence was measured during late exponential phase (ca. 6 h after induction). Anaerobic cells were prepared by transferring the cultures into anoxic conditions and inducing the expression of EcFbFP with 3-*m*B as explained above. Cells were incubated under anoxic conditions, and the EcFbFP fluorescence was evaluated by flow cytometry after 6 h as detailed in Section 2. The level of EcFbFP fluorescence in aerobic cells was considered to be 100, and the fluorescence of the remaining conditions was normalised to this value. Control experiments (Ctrl.) were conducted using *P. putida* KT2440. Bars represent the mean value of the relative fluorescence $\pm$ standard deviation of duplicate measurements from at least two independent experiments.

Taken together, these results indicate that the overall physiological and metabolic state of the recombinant strain under anoxic conditions was more active when compared to those in the wild-type strain. Consequently, we next decided to evaluate the use of *P. putida* KT2400 carrying both AckA$^{E.\ coli}$ and Pdc-AdhB$^{Z.\ mobilis}$ as a host of biotransformations under conditions with restricted O_2 supply.

3.6. *Pseudomonas putida KT2440 carrying AckA$^{E.\ coli}$ and Pdc-AdhB$^{Z.\ mobilis}$ is a suitable anaerobic host for heterologous haloalkane dehalogenase activities*

1,3-DCP (also known as γ-chloroallylchloride or 1,3-dichloropropylene) is a synthetic haloalkene compound that is not known to be formed naturally (van Dijk, 1974), and it is the major active ingredient of Shell D-D^{TM} and Telone II^{TM}. These commercial products are mixtures of *cis*-1,3-DCP, *trans*-1,3-DCP, and 1,2-dichloropropane, and have been used worldwide in

agriculture as pre-plant soil fumigants for the control of plant–parasitic nematodes (Ibekwe et al., 2001; Roberts and Stoydin, 1976). These xenobiotics represent an important class of carcinogenic water pollutants because their components are very resistant to biological degradation and can easily permeate through soil into groundwater supplies. Haloalkene degradation under anoxic conditions is a rare mechanism of detoxification as compared to oxidative dehalogenation. However, slow *in situ* biodegradation of 1,3-DCP and 1,2-dibromoethane in soil has been observed (Roberts and Stoydin, 1976). The emergence of bacteria able to degrade these organochlorides led to the idea that microorganisms that degrade this type of xenobiotic compound must have assembled their catabolic pathways during the past few decades, possibly by the recruitment of pre-existing enzymes. The Gram-negative bacterium *P. pavonaceae* 170 (formerly known as *Pseudomonas cichorii* 170), isolated from soil that was repeatedly treated with 1,3-DCP as a nematocide, is able to utilise low concentrations of 1,3-DCP as its sole carbon and energy source (Poelarends et al., 1998). The mechanism for 1,3-DCP degradation has been elucidated to some extent (Fig. 7). The first step in 1,3-DCP degradation in *P. pavonaceae* 170 is catalysed by a hydrolytic haloalkane dehalogenase (DhaA, E.C. 3.8.1.5) with broad substrate specificity (Janssen, 2004; Verhagen et al., 1995). The *dhaA* gene was most likely acquired from *Rhodococcus rhodochrous* through a horizontal transfer event (Poelarends et al., 2000), and it is known to be constitutively expressed under oxic conditions in its native context. After two sequential oxidation steps catalysed by an alcohol dehydrogenase and an aldehyde dehydrogenase (Janssen et al., 1987b; Poelarends et al., 1998; 1999), the first intermediate metabolite (3-chloro-2-propene-1-ol) is converted into 3-chloro-2-propenal and finally into 3-chloropropenoic acid. The latter compound is the substrate for a 3-chloroacrylic acid dehalogenase (CaaD, E.C. 3.8.1; composed by CaaD1, the α subunit, and CaaD2, the β subunit; Poelarends et al., 2001), which yields 3-oxopropanoate (malonate semialdehyde). This metabolite can finally enter into the central metabolic pathways upon decarboxylation by a malonate semialdehyde decarboxylase. The hydrolytic dechlorination of 1,3-DCP implies the replacement of the chlorine substituent by a hydroxyl group derived from H_2O; therefore, it represents an O_2-independent mechanism of dehalogenation.

To determine if this pathway for 1,3-DCP metabolism could work under anoxic conditions, we cloned the *dhA*, *caaD*1, and *caaD*2 genes from *P. pavonaceae* 170 as a single transcriptional unit (i.e., AHDO, alkyl halide degradation operon) under the control of the XylS/*Pm* system for heterologous expression in *P. putida* KT2440 (Fig. 8A). Note that use of a modified medium (M9C) was critical for performing the experiments under anoxic conditions. One of the recombinants showing the highest activity in microtiter plate assays (Fig. 8B) was selected for *in vitro* quantification of the haloalkane dehalogenase activity in cell-free extracts. Upon induction of AHDO transcription with 3-*m*B, a clear shift was observed in the enzymatic activity (Fig. 8C), which increased to $(1352 \pm 95) \times 10^{-3}$ units mg protein^{-1}, a 2.9-fold increase as compared to non-induced conditions ($P < 0.05$, ANOVA). The background activity detected accounted for $< 125 \times 10^{-3}$ units mg protein^{-1} (i.e., a 12-fold lower level than that observed in induced cultures), which can be at least partially attributed to unspecific reactivity towards residual chloride in the reagents and materials used for the determinations. We also observed significant haloalkane dehalogenase activity in the presence of 1-chlorobutane as the organohalide substrate (data not shown), underscoring the broad range of substrate specificities of DhaA.

Taken together, these results confirm the successful expression of the *dhaA* and *caaD*1/*caaD*2 genes transplanted from *P. pavonaceae* 170 and prompted us to explore the capabilities

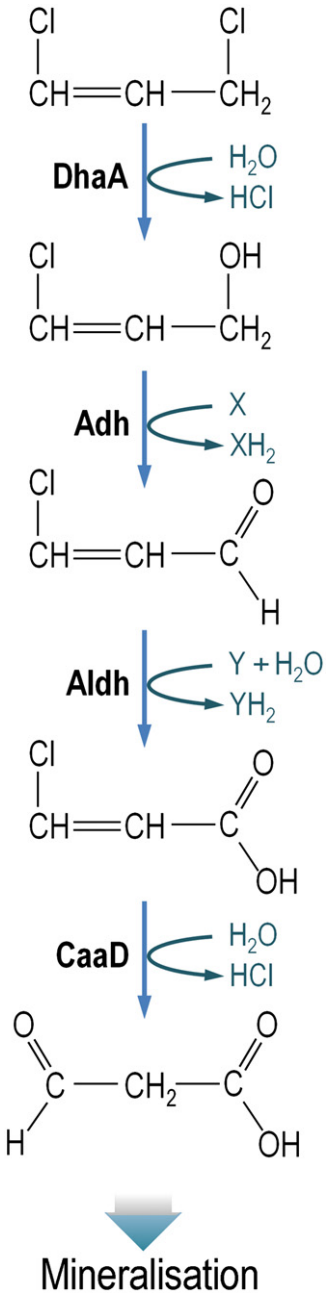

Fig. 7. Biochemical pathway for 1,3-dichloroprop-1-ene biodegradation in the Gram-negative bacterium *P. pavonaceae* 170. The first step is catalyzed by a hydrolytic haloalkane dehalogenase (DhaA, E.C. 3.8.1.5) with broad substrate specificity. After two sequential oxidation steps catalyzed by an alcohol dehydrogenase (Adh) and an aldehyde dehydrogenase (Aldh), the first intermediate metabolite (3-chloro-2-propene-1-ol) is converted into 3-chloro-2-propenal and finally into 3-chloropropenoic acid. Components *X* and *Y* represent electron acceptors that have not been identified yet. The later compound is the substrate for a 3-chloroacrylic acid dehalogenase (CaaD, E.C. 3.8.1; composed by CaaD1, the α subunit, and CaaD2, the β subunit), that yields 3-oxopropanoate (malonate semialdehyde). This metabolite can finally enter into the central metabolic pathways upon decarboxylation by a malonate semialdehyde decarboxylase. As the hydrolytic dechlorination of 1,3-dichloroprop-1-ene implies the replacement of the chlorine substituent by a hydroxyl group derived from two H_2O molecules, it constitutes an O_2-independent mechanism of dehalogenation.

of *P. putida* KT2440 recombinants carrying both AckA$^{E.\ coli}$ and Pdc-AdhB$^{Z.\ mobilis}$ as biocatalysts to be used under anoxic conditions. For this, we co-transformed the expression plasmids containing *ackA*$^{E.\ coli}$ and *pdc-adhB*$^{Z.\ mobilis}$ and AHDO into *P. putida* KT2440 and, after inducing the expression of the genes carried on

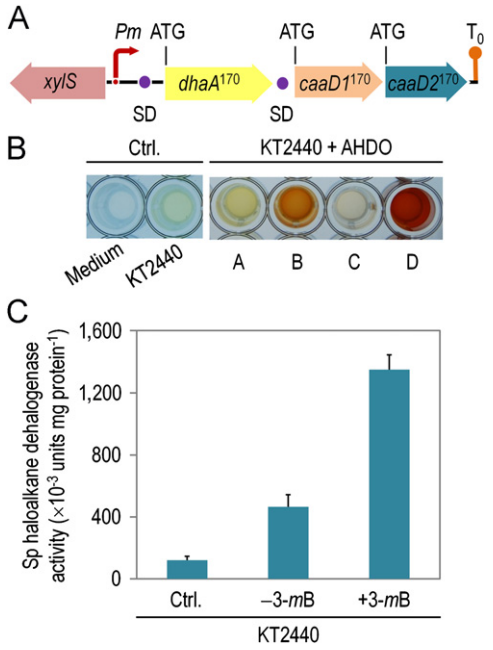

Fig. 8. Introduction of an organohalide biodegradation pathway in *P. putida* KT2440 composed of enzymes from *P. pavonaceae* 170. (A) Schematic representation of the synthetic operon in which *dhaA*^{170}, *caaD*1^{170}, and *caaD*2^{170} are placed under control of an inducible XylS/*Pm* element as a single transcriptional unit. The *dhaA*^{170} and *caaD*1-*caaD*2^{170} coding sequences were preceded by a Shine–Dalgarno (SD) motif, and the transcriptional terminator of the bacteriophage λ is depicted as T_0. The synthetic construct was termed AHDO (alkyl halide degradation operon). The elements in this outline are not drawn to scale. (B) *In vitro* screening of haloalkane dehalogenase activity in selected clones of KT2440 carrying AHDO. M9C, a modified M9 minimal medium with low chloride content, and *P. putida* KT2440 carrying the empty vector, were included to evaluate the background signal in control conditions. (C) *In vitro* quantification of the specific (Sp) haloalkane dehalogenase activity in a selected clone of *P. putida* KT2440 carrying AHDO that gave the highest signal during the screening step. The AHDO expression was induced in all cases by addition of 2.5 mM 3-methylbenzoate (3-*m*B). Control experiments (Ctrl.) were conducted using *P. putida* KT2440 carrying the empty vector. Bars represent the mean value of the specific enzymatic activity ± standard deviation of triplicate measurements from at least two independent experiments.

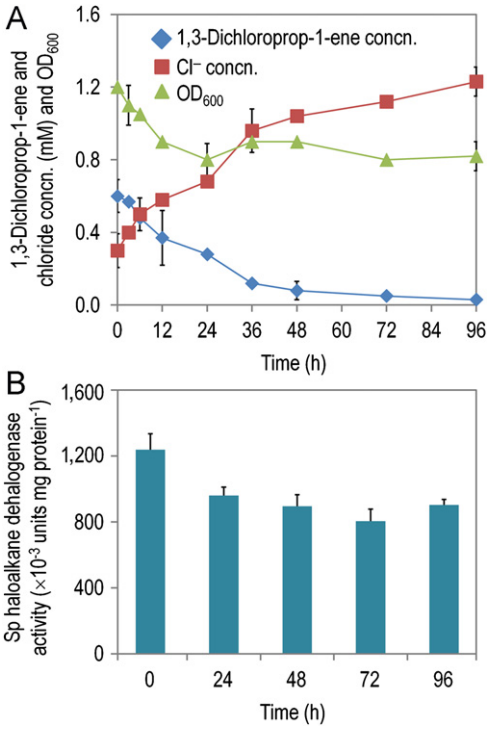

Fig. 9. Anoxic biodegradation of 1,3-dichloroprop-1-ene by a recombinant strain of *P. putida* KT2440. (A) A recombinant derivative of *P. putida* KT2440 carrying AckA$^{E.\ coli}$, Pdc-AdhB$^{Z.\ mobilis}$, and DhaA-CaaD1-CaaD2^{170} (AHDO, alkyl halide degradation operon) was exposed to 0.5 mM 1,3-dichloroprop-1-ene after induction of the heterologous gene expression, and incubated under anoxic conditions in M9C, a modified M9 minimal medium with low chloride content. The kinetics of organohalide biodegradation, evaluated as the residual concentration (concn.) of the compound, was followed by headspace gas chromatography coupled to mass spectrometry. The cell density [estimated as the optical density measured at 600 nm (OD_{600}) of appropriate culture dilutions] and the free chloride concentration were evaluated in these cultures. See Section 2 for further experimental details. (B) *In vitro* quantification of the specific (Sp) haloalkane dehalogenase activity throughout the experiment. Each data point or bar represents the mean value of the corresponding parameter ± standard deviation of duplicate measurements from at least two independent experiments.

the recombinant plasmids, we exposed the cells to 0.5 mM 1,3-DCP under O_2-limited conditions. The biomass concentration in the biodegradation assay, as determined by periodic measurements of the OD_{600}, did not vary significantly over the whole incubation period (96 h; Fig. 9A), thus suggesting that the cells remained viable under these conditions. In fact, a PI-staining assay conducted with cells harvested at 96 h demonstrated that $>50\%$ of the bacterial population excluded the probe, indicating that the recombinant cells were fit under anoxic conditions. The stress imposed on the cells by the addition of the organohalide itself (Loza-Tavera and de Lorenzo, 2011) could also account, at least partially, for the slight decrease in OD_{600} over the course of the biodegradation assay.

After a relatively short lag phase (ca. 4 h), the 1,3-DCP concentration in the culture medium started to decrease and sharply trended downwards over the entire incubation period (Fig. 9A). The highest rate of 1,3-DCP degradation took place during the first 48 h of anoxic incubation; at that point, the residual concentration of 1,3-DCP reached 0.08 mM, representing an 87% clearance of the organohalide. During this period, the specific rate of 1,3-DCP degradation reached 12 ± 3 μmol organohalide h^{-1}, and slowed down towards the end of the incubation period. At the end of the experiment, $>95\%$ of the initial 1,3-DCP was processed by the recombinant *P. putida* strain. The free chloride ion concentration was also measured in the culture supernatants to quantify the haloalkane dehalogenase-mediated liberation of inorganic chloride from the substrate. As expected, the free chloride concentration in the medium increased as the 1,3-DCP concentration decreased in an almost stoichiometric fashion (Fig. 9A), following a trend inversely proportional to that observed for the trajectory of residual organohalide concentration. As a further confirmation of the activity of the recombinant as an organochloride degrader, we also measured the levels of haloalkane dehalogenase activity during the entire incubation period (Fig. 9B). After 96 h, the specific activity decreased to $(903 \pm 34) \times 10^{-3}$ units mg $protein^{-1}$, which is 1.3-fold lower than that observed when cells were first exposed to 1,3-DCP. This change in the enzymatic activity followed the slight decrease in the biomass concentration and could be related to the stressed state of the cells upon exposure to 1,3-DCP or its degradation intermediates. Although lower, this level of haloalkane dehalogenase activity still supported very active organohalide degradation.

A control experiment was conducted with a *P. putida* KT2440 recombinant carrying the empty pSEVA234 vector, the plasmid used for the expression of *ackA*$^{E.\ coli}$ and *pdc-adhB*$^{Z.\ mobilis}$, and equipped with the haloalkane dehalogenase genes from *P. pavonaceae* 170. Noticeably, this strain was unable to thrive under anoxic conditions, and in consequence no 1,3-DCP nor haloalkane dehalogenase activity were detected in this control experiment. Moreover, *P. pavonaceae* 170, the source of the

haloalkane dehalogenase genes, is also unable to thrive under anoxic conditions.

4. Conclusions

Advances in biocatalysis are key to reducing the environmental footprint of chemical processes, especially petroleum-based technologies (Demain, 2009). In this context, biotechnological processes conducted under conditions with restricted O_2 supply are becoming of increasing interest for both *in situ* and *ex situ* treatments. The results above show that a rational metabolic engineering approach can expand the range of niches and sites that can be targeted by modified *P. putida* strains and related bacteria. Although genetic programming of anaerobes is still a difficult endeavour, one can envision the wealth of molecular tools and conceptual frames offered by contemporary Systems and Synthetic Biology approaches for designing biological agents that can operate in a wide range of redox conditions. Recent advances within this framework have been promissory (Boyle and Silver, 2012; Bujara and Panke, 2010), and will certainly lead to significant improvements in the field of metabolic engineering (Yadav et al., 2012).

The whole-cell catalyst designed in this work consisted of *P. putida* as the *chassis* and genes recruited from three different bacteria that altered the metabolic state of the cells at the ATP and NADH level and allowed the degradation of 1,3-DCP in anaerobiosis. The lack of growth of this metabolically re-factored strain in cultures deprived of O_2 is in reality an asset and not a liability because the optimal environmental catalyst is the one that displays maximum activity with minimum biomass generation. In our study, the new metabolic properties of the recombinant *P. putida* strain allowed it to survive and effectively execute the desired reaction in the absence of O_2 over a substantial period of time. Further improvements of these biocatalysts can be anticipated by considering the stress response of the microorganisms when exposed to organohalides, an important (and certainly unavoidable) hurdle that bacteria have to face in the biodegradation processes. It has been recently shown that the core metabolism of *P. putida* KT2440 possesses a remarkable buffering capacity and a high flexibility for counteracting different metabolic perturbations without displaying a distinct phenotype (Ebert et al., 2011). Future attempts to move the environmental window of *P. putida* towards strictly anoxic conditions may focus on metabolic modifications that directly couple oxidation of hexoses to NADH regeneration and ATP production, ideally without formation of by-products (that could act as toxic/stress agents themselves). In spite of the restrictions imposed by the properties of the central catabolic pathways in pseudomonads, the present work represents a first case study toward shifting the metabolic system of *P. putida* towards lower redox potentials, thereby further increasing the intrinsic value of this microorganism as a bioremediation and biotransformation agent.

Acknowledgments

The authors wish to thank Prof. Dick B. Janssen (Institute for Biomolecular Sciences and Biotechnology, Groningen, The Netherlands) for the kind gift of *Pseudomonas pavonaceae* 170, and Dr. Thomas Drepper (Institute for Molecular Enzyme Technology, Jülich, Germany) for generously sharing the EcFbFP protein. This study was supported by the BIO and FEDER CONSOLIDER-INGENIO programme of the Spanish Ministry of Science and Innovation, the BACSINE, MICROME, and ST-FLOW Contracts of the EU, and the PROMT Project of the CAM. PIN is a researcher from the Consejo Nacional de Investigaciones Científicas y Técnicas (Argentina) and holds an EMBO Long-Term Fellowship (ALTF 13-2010).

Appendix A. Supporting information

Supplementary data associated with this article can be found in the online version at http://dx.doi.org/10.1016/j.ymben.2012.09.006.

References

Abril, M.A., Michan, C., Timmis, K.N., Ramos, J.L., 1989. Regulator and enzyme specificities of the TOL plasmid-encoded upper pathway for degradation of aromatic hydrocarbons and expansion of the substrate range of the pathway. J. Bacteriol. 171, 6782–6790.

Andersen, K.B., von Meyenburg, K., 1977. Charges of nicotinamide adenine nucleotides and adenylate energy charge as regulatory parameters of the metabolism in *Escherichia coli*. J. Biol. Chem. 252, 4151–4156.

Arai, H., 2011. Regulation and function of versatile aerobic and anaerobic respiratory metabolism in *Pseudomonas aeruginosa*. Front. Microbiol. 2, 103.

Baba, T., Ara, T., Hasegawa, M., Takai, Y., Okumura, Y., Baba, M., Datsenko, K.A., Tomita, M., Wanner, B.L., Mori, H., 2006. Construction of *Escherichia coli* K-12 in-frame, single-gene knockout mutants: the Keio collection. Mol. Syst. Biol. 2 2006.0008.

Bagdasarian, M., Lurz, R., Rückert, B., Franklin, F.C.H., Bagdasarian, M.M., Frey, J., Timmis, K.N., 1981. Specific purpose plasmid cloning vectors. II. Broad host range, high copy number, RSF1010-derived vectors, and a host-vector system for gene cloning in *Pseudomonas*. Gene 16, 237–247.

Belkin, S., 1992. Biodegradation of haloalkanes. Biodegradation 3, 299–313.

Bergmann, J.G., Sanik, J., 1957. Determination of trace amounts of chlorine in naphtha. Anal. Chem. 29, 241–243.

Blank, L.M., Ionidis, G., Ebert, B.E., Bühler, B., Schmid, A., 2008. Metabolic response of *Pseudomonas putida* during redox biocatalysis in the presence of a second octanol phase. FEBS J. 275, 5173–5190.

Blattner, F.R., Plunkett 3rd, G., Bloch, C.A., Perna, N.T., Burland, V., Riley, M., Collado-Vides, J., Glasner, J.D., Rode, C.K., Mayhew, G.F., Gregor, J., Davis, N.W., Kirkpatrick, H.A., Goeden, M.A., Rose, D.J., Mau, B., Shao, Y., 1997. The complete genome sequence of *Escherichia coli* K-12. Science 277, 1453–1462.

Bothast, R.J., Nichols, N.N., Dien, B.S., 1999. Fermentations with new recombinant organisms. Biotechnol. Progr. 15, 867–875.

Boyer, H.W., Roulland-Dussoix, D., 1969. A complementation analysis of the restriction and modification of DNA in *Escherichia coli*. J. Mol. Biol. 41, 459–472.

Boyle, P.M., Silver, P.A., 2012. Parts plus pipes: synthetic biology approaches to metabolic engineering. Metab. Eng. 14, 223–232.

Bradford, M.M., 1976. A rapid and sensitive method for the quantitation of microgram quantities of protein utilizing the principle of protein-dye binding. Anal. Biochem. 72, 248–254.

Bringer-Meyer, S., Schimz, K.L., Sahm, H., 1986. Pyruvate decarboxylase from *Zymomonas mobilis*. Isolation and partial characterization. Arch. Microbiol. 146, 105–110.

Brown, T.D.K., Jones-Mortimer, M.C., Kornberg, H.L., 1977. The enzymic interconversion of acetate and acetyl-coenzyme A in *Escherichia coli*. Microbiology 102, 327–336.

Bujara, M., Panke, S., 2010. Engineering in complex systems. Curr. Opin. Biotechnol. 21, 586–591.

Byun, M.O.K., Kaper, J.B., Ingram, L.O., 1986. Construction of a new vector for the expression of foreign genes in *Zymomonas mobilis*. J. Ind. Microbiol. 1, 9–15.

Castro, C.E., 1977. Biodehalogenation. Environ. Health Perspect. 21, 279–283.

Chapman, A.G., Fall, L., Atkinson, D.E., 1971. Adenylate energy charge in *Escherichia coli* during growth and starvation. J. Bacteriol. 108, 1072–1086.

Chavarría, M., Kleijn, R.J., Sauer, U., Pflüger-Grau, K., de Lorenzo, V., 2012. Regulatory tasks of the phosphoenolpyruvate-phosphotransferase system of *Pseudomonas putida* in central carbon metabolism. mBio 3, e00028–12.

Clark, D.P., 1989. The fermentation pathways of *Escherichia coli*. FEMS Microbiol. Rev. 5, 223–234.

Coder, D.M., 1997. Assessment of bacterial viability status by flow cytometry and single cell sorting. Curr. Protoc. Cytom. 15, 9.2.1–9.2.14.

Conway, T., 1992. The Entner–Doudoroff pathway: history, physiology and molecular biology. FEMS Microbiol. Rev. 103, 1–27.

Demain, A.L., 2009. Biosolutions to the energy problem. J. Ind. Microbiol. Biotechnol. 36, 319–332.

de Graef, M.R., Alexeeva, S., Snoep, J.L., Teixeira de Mattos, M.J., 1999. The steady-state internal redox state (NADH/NAD) reflects the external redox state and is correlated with catabolic adaptation in *Escherichia coli*. J. Bacteriol. 181, 2351–2357.

de Jong, R.M., Dijkstra, B.W., 2003. Structure and mechanism of bacterial dehalogenases: different ways to cleave a carbon–halogen bond. Curr. Opin. Struct. Biol. 13, 722–730.

de Lorenzo, V., Timmis, K.N., 1994. Analysis and construction of stable phenotypes in gram-negative bacteria with Tn*5*- and Tn*10*-derived minitransposons. Methods Enzymol . 235, 386–405.

Diefenbach, R.J., Duggleby, R.G., 1991. Pyruvate decarboxylase from *Zymomonas mobilis*. Structure and re-activation of apoenzyme by the cofactors thiamin diphosphate and magnesium ion. Biochem. J. 276, 439–445.

Dittrich, C.R., Bennett, G.N., San, K.Y., 2005. Characterization of the acetate-producing pathways in *Escherichia coli*. Biotechnol. Progr. 21, 1062–1067.

Drepper, T., Eggert, T., Circolone, F., Heck, A., Kraub, U., Guterl, J.K., Wendorff, M., Losi, A., Gärtner, W., Jaeger, K.E., 2007. Reporter proteins for *in vivo* fluorescence without oxygen. Nat. Biotechnol. 25, 443–445.

Drepper, T., Huber, R., Heck, A., Circolone, F., Hillmer, A.K., Büchs, J., Jaeger, K.E., 2010. Flavin mononucleotide-based fluorescent reporter proteins outperform green fluorescent protein-like proteins as quantitative *in vivo* real-time reporters. Appl. Environ. Microbiol. 76, 5990–5994.

Duque, E., Molina-Henares, A.J., de la Torre, J., Molina-Henares, M.A., del Castillo, T., Lam, J., Ramos, J.L., 2007. Towards a genome-wide mutant library of *Pseudomonas putida* strain KT2440. In: Ramos, J.L., Filloux, A. (Eds.), *Pseudomonas*: A Model System in Biology, 5. Springer, DE, Berlin, pp. 227–251.

Ebert, B.E., Kurth, F., Grund, M., Blank, L.M., Schmid, A., 2011. Response of *Pseudomonas putida* KT2440 to increased NADH and ATP demand. Appl. Environ. Microbiol. 77, 6597–6605.

Eschbach, M., Schreiber, K., Trunk, K., Buer, J., Jahn, D., Schobert, M., 2004. Long-term anaerobic survival of the opportunistic pathogen *Pseudomonas aeruginosa* via pyruvate fermentation. J. Bacteriol. 186, 4596–4604.

Fetzner, S., 1998. Bacterial dehalogenation. Appl. Microbiol. Biotechnol. 50, 633–657.

Fuhrer, T., Fischer, E., Sauer, U., 2005. Experimental identification and quantification of glucose metabolism in seven bacterial species. J. Bacteriol. 187, 1581–1590.

Geddes, C.C., Nieves, I.U., Ingram, L.O., 2011. Advances in ethanol production. Curr. Opin. Biotechnol. 22, 312–319.

Häggblom, M.M., Young, L.Y., 1999. Anaerobic degradation of 3-halobenzoates by a denitrifying bacterium. Arch. Microbiol. 171, 230–236.

Häggblom, M.M., Knight, V.K., Kerkhof, L.J., 2000. Anaerobic decomposition of halogenated aromatic compounds. Environ. Pollut. 107, 199–207.

Hanahan, D., Meselson, M., 1983. Plasmid screening at high colony density. Methods Enzymol. 100, 333–342.

Hartmanis, M.G.N., Gatenbeck, S., 1984. Intermediary metabolism in *Clostridium acetobutylicum*: levels of enzymes involved in the formation of acetate and butyrate. Appl. Environ. Microbiol. 47, 1277–1283.

Hayashi, T., Kato, T., Furukawa, K., 2012. Respiratory chain analysis of *Zymomonas mobilis* mutants producing high levels of ethanol. Appl. Environ. Microbiol. 78, 5622–5629.

Herrero, M., de Lorenzo, V., Timmis, K.N., 1990. Transposon vectors containing non-antibiotic resistance selection markers for cloning and stable chromosomal insertion of foreign genes in gram-negative bacteria. J. Bacteriol. 172, 6557–6567.

Hoppner, T.C., Doelle, H.W., 1983. Purification and kinetic characteristics of pyruvate decarboxylase and ethanol dehydrogenase from *Zymomonas mobilis* in relation to ethanol production. Appl. Microbiol. Biotechnol. 17, 152–157.

Horton, R.M., Cai, Z.L., Ho, S.N., Pease, L.R., 1990. Gene splicing by overlap extension: tailor-made genes using the polymerase chain reaction. BioTechniques 8, 528–535.

Ibekwe, A.M., Papiernik, S.K., Yates, S.R., Crowley, D.E., Yang, C.H., 2001. Microcosm enrichment of 1,3-dichloropropene-degrading soil microbial communities in a compost-amended soil. J. Appl. Microbiol. 91, 668–676.

Janssen, D.B., 2004. Evolving haloalkane dehalogenases. Curr. Opin. Chem. Biol. 8, 150–159.

Janssen, D.B., Jager, D., Witholt, B., 1987a. Degradation of *n*-haloalkanes and α, ω-dihaloalkanes by wild-type and mutants of *Acinetobacter* sp. strain GJ70. Appl. Environ. Microbiol. 53, 561–566.

Janssen, D.B., Keuning, S., Witholt, B., 1987b. Involvement of a quinoprotein alcohol dehydrogenase and an NAD-dependent aldehyde dehydrogenase in 2-chloroethanol metabolism in *Xanthobacter autotrophicus* GJIO. J. Gen. Microbiol. 133, 85–92.

Janssen, D.B., Oppentocht, J.E., Poelarends, G.J., 2001. Microbial dehalogenation. Curr. Opin. Biotechnol. 12, 254–258.

Kanehisa, M., Goto, S., Sato, Y., Furumichi, M., Tanabe, M., 2012. KEGG for integration and interpretation of large-scale molecular data sets. Nucleic Acids Res. 40, D109–D114.

Keseler, I.M., Collado-Vides, J., Santos-Zavaleta, A., Peralta-Gil, M., Gama-Castro, S., Muñiz-Rascado, L., Bonavides-Martinez, C., Paley, S., Krummenacker, M., Altman, T., Kaipa, P., Spaulding, A., Pacheco, J., Latendresse, M., Fulcher, C., Sarker, M., Shearer, A.G., Mackie, A., Paulsen, I., Gunsalus, R.P., Karp, P.D., 2011. EcoCyc: a comprehensive database of *Escherichia coli* biology. Nucleic Acids Res. 39, D583–D590.

Kessler, B., Herrero, M., Timmis, K.N., de Lorenzo, V., 1994. Genetic evidence that the XylS regulator of the *Pseudomonas* TOL meta operon controls the *Pm* promoter through weak DNA-protein interactions. J. Bacteriol. 176, 3171–3176.

Keuning, S., Janssen, D.B., Witholt, B., 1985. Purification and characterization of hydrolytic haloalkane dehalogenase from *Xanthobacter autotrophicus* GJ10. J. Bacteriol. 163, 635–639.

Knappe, J., Sawers, G., 1990. A radical-chemical route to acetyl-CoA: the anaerobically induced pyruvate formate-lyase system of *Escherichia coli*. FEMS Microbiol. Rev. 75, 383–398.

Lee, M.D., Odom, J.M., Buchanan Jr., R.J., 1998. New perspectives on microbial dehalogenation of chlorinated solvents: insights from the field. Annu. Rev. Microbiol. 52, 423–452.

Loza-Tavera, H., de Lorenzo, V., 2011. Microbial bioremediation of chemical pollutants: how bacteria cope with multi-stress environmental scenarios. In: Storz, R., Hengge, R. (Eds.), Bacterial Stress Responses. ASM Press, Washington, DC, pp. 481–492.

Lundin, A., Hasenson, M., Persson, J., Pousette, Å., 1986. Estimation of biomass in growing cell lines by adenosine triphosphate assay. Methods Enzymol. 133, 27–42.

Neale, A.D., Scopes, R.K., Kelly, J.M., Wettenhall, R.E.H., 1986. The two alcohol dehydrogenases of *Zymomonas mobilis*. Purification by differential dye ligand chromatography, molecular characterisation and physiological roles. Eur. J. Biochem. 154, 119–124.

Nelson, K.E., Weinel, C., Paulsen, I.T., Dodson, R.J., Hilbert, H., Martins dos Santos, V.A.P., Fouts, D.E., Gill, S.R., Pop, M., Holmes, M., Brinkac, L., Beanan, M., DeBoy, R.T., Daugherty, S., Kolonay, J., Madupu, R., Nelson, W., White, O., Peterson, J., Khouri, H., Hance, I., Chris Lee, P., Holtzapple, E., Scanlan, D., Tran, K., Moazzez, A., Utterback, T., Rizzo, M., Lee, K., Kosack, D., Moestl, D., Wedler, H., Lauber, J., Stjepandic, D., Hoheisel, J., Straetz, M., Heim, S., Kiewitz, C., Eisen, J.A., Timmis, K.N., Düsterhöft, A., Tümmler, B., Fraser, C.M., 2002. Complete genome sequence and comparative analysis of the metabolically versatile *Pseudomonas putida* KT2440. Environ. Microbiol. 4, 799–808.

Neumann, G., Cornelissen, S., van Breukelen, F., Hunger, S., Lippold, H., Loffhagen, N., Wick, L.Y., Heipieper, H.J., 2006. Energetics and surface properties of *Pseudomonas putida* DOT-T1E in a two-phase fermentation system with 1-decanol as second phase. Appl. Environ. Microbiol. 72, 4232–4238.

Nikel, P.I., de Lorenzo, V., 2012. Implantation of unmarked regulatory and metabolic modules in gram-negative bacteria with specialised mini-transposon delivery vectors. J. Biotechnol. , http://dx.doi.org/10.1016/j.jbiotec.2012.05.002, In press.

Nilsson, T., Schultz, V., Berggren, P.O., Corkey, B.E., Tornheim, K., 1996. Temporal patterns of changes in ATP/ADP ratio, glucose 6-phosphate and cytoplasmic free Ca^{2+} in glucose-stimulated pancreatic β-cells. Biochem. J. 314, 91–94.

Nogales, J., Palsson, B.Ø., Thiele, I., 2008. A genome-scale metabolic reconstruction of *Pseudomonas putida* KT2440: *i*JN746 as a cell factory. BMC Syst. Biol. 2, 79.

Ohta, K., Beall, D.S., Mejia, J.P., Shanmugam, K.T., Ingram, L.O., 1991. Genetic improvement of *Escherichia coli* for ethanol production: chromosomal integration of *Zymomonas mobilis* genes encoding pyruvate decarboxylase and alcohol dehydrogenase II. Appl. Environ. Microbiol. 57, 893–900.

Poblete-Castro, I., Becker, J., Dohnt, K., Martins dos Santos, V.A.P., Wittmann, C., 2012. Industrial biotechnology of *Pseudomonas putida* and related species. Appl. Microbiol. Biotechnol. 93, 2279–2290.

Poelarends, G.J., Wilkens, M., Larkin, M.J., van Elsas, J.D., Janssen, D.B., 1998. Degradation of 1,3-dichloropropene by *Pseudomonas cichorii* 170. Appl. Environ. Microbiol. 64, 2931–2936.

Poelarends, G.J., van Hylckama Vlieg, J.E.T., Marchesi, J.R., Freitas dos Santos, L.M., Janssen, D.B., 1999. Degradation of 1,2-dibromoethane by *Mycobacterium sp.* strain GP1. J. Bacteriol. 181, 2050–2058.

Poelarends, G.J., Kulakov, L.A., Larkin, M.J., van Hylckama Vlieg, J.E.T., Janssen, D.B., 2000. Roles of horizontal gene transfer and gene integration in evolution of 1,3-dichloropropene- and 1,2-dibromoethane-degradative pathways. J. Bacteriol. 182, 2191–2199.

Poelarends, G.J., Saunier, R., Janssen, D.B., 2001. *Trans*-3-chloroacrylic acid dehalogenase from *Pseudomonas pavonaceae* 170 shares structural and mechanistic similarities with 4-oxalocrotonate tautomerase. J. Bacteriol., 183.

Puchalka, J., Oberhardt, M.A., Godinho, M., Bielecka, A., Regenhardt, D., Timmis, K.N., Papin, J.A., Martins dos Santos, V.A.P., 2008. Genome-scale reconstruction and analysis of the *Pseudomonas putida* KT2440 metabolic network facilitates applications in biotechnology. PLoS Comput. Biol. 4, e1000210.

Roberts, T.R., Stoydin, G., 1976. The degradation of (*Z*)- and (*E*)-1,3-dichloropropenes and 1,2-dichloropropane in soil. Pestic. Sci. 7, 325–335.

Sambrook, J., Russell, D.W., 2001. Molecular cloning: a laboratory manual. Cold Spring Harbor Laboratory. Cold Spring Harbor.

Sawers, G., Böck, A., 1988. Anaerobic regulation of pyruvate formate-lyase from *Escherichia coli* K-12. J. Bacteriol. 170, 5330–5336.

Schöler, H.F., Keppler, F., Fahimi, I.J., Niedan, V.W., 2003. Fluxes of trichloroacetic acid between atmosphere, biota, soil, and groundwater. Chemosphere 52, 339–354.

Schultz, V., Sussman, I., Bokvist, K., Tornheim, K., 1993. Bioluminometric assay of ADP and ATP at high ATP/ADP ratios: assay of ADP after enzymatic removal of ATP. Anal. Biochem. 215, 302–304.

Shiro, Y., Sugimoto, H., Tosha, T., Nagano, S., Hino, T., 2012. Structural basis for nitrous oxide generation by bacterial nitric oxide reductases. Philos. Trans. R. Soc. London, Ser. B 367, 1195–1203.

Silva-Rocha R., Martínez-García E., Calles B., Chavarría M., Arce-Rodríguez A., de las Heras A., Páez-Espino D., Durante-Rodríguez G., Kim J., Nikel P.I., Platero R., de Lorenzo V. The Standard European Vector Architecture (SEVA): a coherent platform for the analysis and deployment of complex prokaryotic phenotypes. Nucl. Acids Res., (in press).

Sohn, S.B., Kim, T.Y., Park, J.M., Lee, S.Y., 2010. *In silico* genome-scale metabolic analysis of *Pseudomonas putida* KT2440 for polyhydroxyalkanoate synthesis, degradation of aromatics and anaerobic survival. Biotechnol. J. 5, 739–750.

Song, B.K., Palleroni, N.J., Häggblom, M.M., 2000. Isolation and characterization of diverse halobenzoate-degrading denitrifying bacteria from soils and sediments. Appl. Environ. Microbiol. 66, 3446–3453.

Verdoni, N., Aon, M.A., Lebeault, J.M., 1992. Metabolic and energetic control of *Pseudomonas mendocina* growth during transitions from aerobic to oxygen-limited conditions in chemostat cultures. Appl. Environ. Microbiol. 58, 3150–3156.

Verhagen, C., Smit, E., Janssen, D.B., van Elsas, J.D., 1995. Bacterial dichloropropene degradation in soil; screening of soils and involvement of plasmids carrying the *dhlA* gene. Soil Biol. Biochem. 27, 1547–1557.

van Dijk, H., 1974. Degradation of 1,3-dichloropropenes in the soil. AgroEcosystems 1, 193–204.

Yadav, V.G., De Mey, M., Lim, C.G., Ajikumar, P.K., Stephanopoulos, G., 2012. The future of metabolic engineering and synthetic biology: towards a systematic practice. Metab. Eng. 14, 233–241.